THE UNIVERSITY OF ADELAIDE
School of Earth and Environmental Sciences

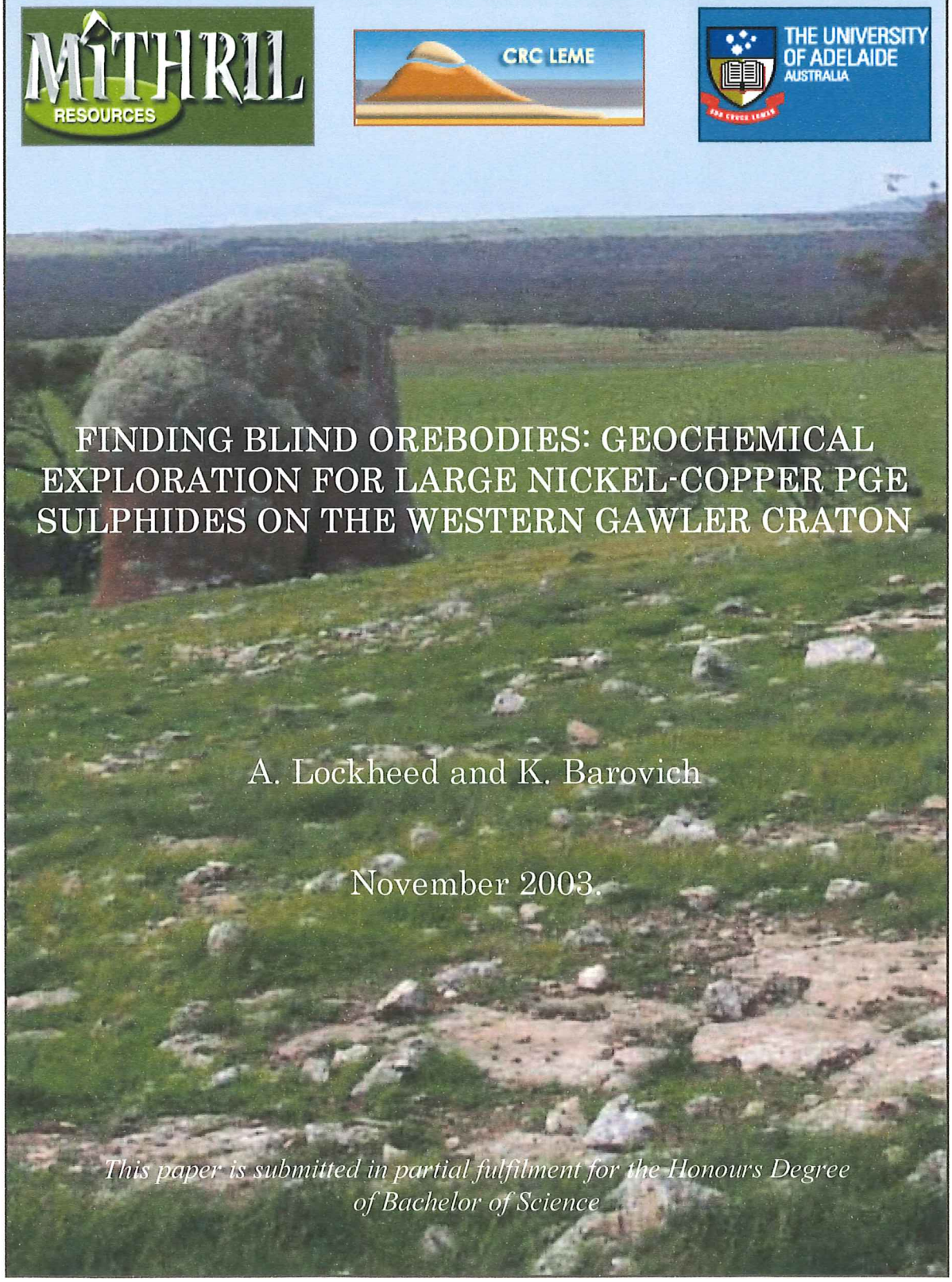

FINDING BLIND OREBODIES: GEOCHEMICAL EXPLORATION FOR LARGE NICKEL-COPPER PGE SULPHIDES ON THE WESTERN GAWLER CRATON

A. Lockheed and K. Barovich

November 2003.

This paper is submitted in partial fulfilment for the Honours Degree of Bachelor of Science

TABLE OF CONTENTS

Finding blind orebodies: geochemical exploration for large nickel-copper and PGE sulphides on the Western Gawler Craton.

A. E. Lockheed
CRC LEME, School of Earth and Environmental Sciences,
The University of Adelaide.

Abstract

The search for economically viable ore deposits focuses increasingly on deeply buried deposits. This study was designed to highlight specific mafic/ultramafic igneous bodies in the western Gawler Craton, near Streaky Bay, South Australia, through the analysis of the behaviour of pathfinder elements within the regolith above anomalous aeromagnetic targets. In particular, the possibility of developing a rapid and inexpensive means of characterising the intrusions at depth by looking within the calcareous sediments located within the top two to twelve metres of regolith was evaluated.

Data from 26 of the 53 holes drilled were analysed, covering an area of approximately 24 km^2. This area covers a diverse lithological basement including ultramafics, gabbros, granitoids and felsic gneisses and is located near a strong magnetic anomaly.

Given the significant difference in basement lithology of the target bodies (mafic to ultramafic) versus the variably magnetic felsic to intermediate granitoids, pathfinder elements including Ni, Cu, Cr, Mn and V, which are elevated in mafic to ultramafic rocks, were targeted. Depth plots and ratios of the transition elements are shown with simple graphing techniques are used to illustrate the behaviour of geochemical signatures throughout the profile and to display any correlation between basement rocks and the regolith.

There was no discernible anomaly in any trace metals throughout the calcrete of the uppermost regolith unit. Calcrete pathfinder element abundances are uniformly low, which is to be expected, as the sediments are up to 75% carbonate, and any basement detrital signature is highly diluted. In the majority of holes, however, an abrupt increase in these element values occurred at the base of the calcrete or a few metres deeper within ferruginous sediments. The increase in values occurred in Ni, Cu and Cr, but was most prominent in V. This pattern is reflected in the plots for the basement saprolitic material.

Unfortunately, sampling of the oxidised zones requires expensive and time-consuming air-core drilling through up to twelve metres of calcrete, and in places soft, unconsolidated sands. More detailed geochemical analyses of the calcrete layers in the 26 holes were undertaken to try to establish a method of identifying the basement lithology from the calcrete chemical data. Absolute abundances of pathfinder elements are too low in the calcrete to be useful in distinguishing differences in basement lithology.

While calcareous sediments may contain subtle geochemical indicators of the differences in basement lithology, it alone is not adequate to confidently predict the basement lithology for drilling. Below the calcrete, within the oxidised zone, the geochemical anomalies are large enough to confidently conclude whether the basement is mafic or felsic.

Keywords: Gawler Craton, pathfinder elements, geochemical signatures, regolith, ferruginous sediments.

---

1. Introduction

In Australia, where over 70% of the continent is regolith-dominated, exploration under and within cover is an enduring challenge. While drill hole sampling is a major regional exploration tool, it is expensive and regolith geochemical sampling can be a desirable alternative, although the regolith geochemical signature of ore bodies at depth is likely to be weak and difficult to interpret.

Outcrop on the western Gawler Craton is limited so the majority of the basement has been interpreted from drill hole and aeromagnetic data (Ferris *et al.*, 2002). Basement rocks of the Streaky Bay area, south-western Eyre Peninsula, are deformed Palaeoproterozoic sedimentary and igneous rocks into which deformed Palaeoproterozoic granitoids of the 1630 Ma St. Peter Suite are intruded (Parker, 1993a). Undeformed Mesoproterozoic Hiltaba Suite Granites and the Gawler Range Volcanics are likely to be the youngest units of the basement. Mafic to ultramafic intrusive complexes of unknown stratigraphic position and age also occur within the basement. They have been intersected in numerous drill holes and are believed to be responsible for at least some of the magnetic and gravity anomalies seen throughout the region (WMC, 1995).

A complicated stratigraphy of Tertiary and Quaternary sediments covers the Streaky Bay area. Fine to gravely sand, silts and clays of the Pidinga and Garford Formations are incorporated within and overlain by ferricrete horizons. The Quaternary Bridgewater Formation contains calcareous silts and aeolinites and forms a relatively hard cap over the Tertiary sediments (Rankin and Flint, 1991).

The principal intent of this research is to investigate the potential for differentiating basement lithology from the upper parts of a regolith profile. The effect of weathering on a profile and the common dispersion behaviour of the transition elements, especially nickel and copper, constitute the fundamental concerns of the study. Rattigan *et al.* (1977) and Friedrich and Christensen (1977) completed similar work in the Stuart Shelf, South Australia and Kalgoorlie, Western Australia, respectively.

2. Geological Setting

Regional Geology

The Gawler Craton is an extensive crystalline basement incorporating Archean to Mesoproterozoic metasediments, volcanics and granites (Fig. 1) that have not been subjected to any deformation of considerable significance since 1450 Ma (Thomson, 1975; Parker, 1993a). Three major tectonic and crustal forming events occurred within the Craton during the Late Archean to Mesoproterozoic. The Sleafordian Orogeny (~2700-2300 Ma) was widespread deforming Archean crust in the centre, north and south-east. The recently named Neill event (~1850 Ma) affected the eastern Gawler Craton (Ferris *et al.*, 2002). The Kimban Orogeny (~1730-1700 Ma) occurred throughout the southern and central Gawler Craton. The Kararan Orogeny (~1650-1540 Ma) affected areas in the north and west and possibly created many structures into which Palaeoproterozoic to Mesoproterozoic units were emplaced (Ferris *et al.*, 2002). Younger sediments predominantly conceal the Gawler Craton, so interpretation of its boundaries was attained from total magnetic intensity and gravity data (Daly *et al.*, 1998; Ferris *et al.*, 2002).

The northern and western margins are obscured by sediments of the Neoproterozoic to Phanerozoic Officer Basin, but were clearly identified from a linear geophysical anomaly. The Torrens Hinge Zone emerged during the evolution of the Neoproterozoic Adelaide Geosyncline and forms the Craton's distinct boundaries in the east and south-east. Gravity and magnetic characteristics place the southern limits of the Craton close to the continental shelf, within the Southern Ocean (Ferris *et al.*, 2002). The geology along the margins of the Gawler Craton was inferred from limited outcrop and information from randomly located drill holes (Daly *et al.*, 1998; Ferris *et al.*, 2002).

Regional mapping, isotopic analysis and geochemistry has been used in association with the geophysical data to subdivide the Gawler Craton into several domains of differing structural, metamorphic and stratigraphic characteristics as shown by Thomson (1970) and Parker (1990) (Fig. 2).

Local Geology

Streaky Bay is located on the south-west coast of the Eyre Peninsula, approximately 720 km from Adelaide, South Australia. It is within the lower half of the Nuyts Domain, central Gawler Craton (Fig. 2). The boundaries of the Nuyts Domain in the north with the Wilgena Domain and west with the Fowler Domain are relatively distinct due to the Yerda and Coorabie shear zones respectively (Ferris *et al.*, 2002). It is believed that the Yarlbrinda Shear Zone bounds the eastern margin of the Nuyts Domain but remains difficult to interpret as it is covered by the overlying Gawler Range Volcanics.

The south eastern boundary with the Coulta Domain is particularly questionable and could exist at one of two locations (Stewart and Foden, 2001) (Fig. 2).

Earliest interpretations of the Nuyts Domain proposed that it was primarily Archean basement. Through recent discoveries involving geochronology and isotopic analysis it has been proven to be largely Palaeoproterozoic and of felsic igneous composition (Ferris *et al.*, 2002).

The St. Peter Suite, a deformed magmatic intrusive sequence, was emplaced into the Nuyts Domain between ~1630-1610 Ma. The suite consists of tonalitic to granodioritic rocks, which have similar geochemistry to Archean tonalite-trondhjemite-granodiorite suites (Ferris *et al.*, 2002). Outcrop of the St. Peter Suite occurs along the coast at The Granites, Point Westall and Smooth-Pool south of Streaky Bay, but does not crop out inland (Fig. 3). Two main components occur within the suite. One is a pink, fine to medium-grained, weakly to well-foliated granite grading to a pink-red, medium to coarse-grained granite with microcline and plagioclase phenocrysts up to 30 mm in diameter. The second member is a grey, medium-grained, moderately to well-foliated, granodiorite also exhibiting relatively large plagioclase phenocrysts. Metamorphosed intermediate to mafic and granodiorite dykes occur throughout the suite, typically sub-parallel to the foliations of the major units mentioned above (Rankin and Flint, 1991). St. Peter Suite granites display volcanic arc setting geochemical signatures, although such characteristics may also be created by continental extension and the resultant mantle under-plating (Ferris *et al.*, 2002). A possible explanation for the emplacement of the St. Peter Suite granites is a magmatic arc setting located south west of the Archean basement (in the east of the Gawler Craton), which is associated with north-east dipping subduction (Ferris *et al.*, 2002).

Ca 1580 Ma Hiltaba Suite plutons are ubiquitous across the entire Gawler Craton. In the Nuyts Domain they are associated with the northern and eastern shear zones.

The Hiltaba Suite plutons are both deformed and undeformed which suggests their emplacement could have been partly syn-orogenic, rather than an anorogenic setting as was previously believed (Creaser, 1989; Flint, 1993; Stewart and Foden, 2001). Lithological and mineralogical characteristics of the Hiltaba granitoids differ throughout the Gawler Craton. The Hiltaba Suite seen inland from Streaky Bay would most likely correspond to the Calca Granite, which is a distinctive red, coarse-grained granite (Parker, 1993a). It contains a high percentage of orthoclase and microcline (50-75%) and a much smaller percentage of plagioclase (<5%). It is characterised by fine-grained hematite, which is responsible for its distinguishing colouration. The Hiltaba Suite plutons display a wide variability in geochemistry and Sm-Nd isotope values. The Nuyts Domain Hiltaba granites exhibit positive ε_{Nd} values suggesting a depleted mantle source. Samples east of the Nuyts Domain have negative ε_{Nd} values that may indicate a continental source. This information may suggest a partial mantle source mixed with an Archean crust (Ferris *et al.*, 2002). It has also been suggested that Hiltaba Suite emplacement may be associated with the north-east dipping subduction zone, as part of a back-arc, intracontinental environment (Ferris *et al.*, 2002).

The Gawler Range Volcanics were comagmatically emplaced with the Hiltaba Suite plutons (~1595-1575 Ma). They form a bimodal volcanic province that crops out in an area greater than 25 000 km^2 (Fig. 1) (Daly *et al.*, 1998). The main exposures of the volcanics are located approximately 100 km north-east of Streaky Bay. Basalt-dacite-rhyodacite-rhyolite assemblages of pyroclastic rocks shape the Gawler Range Volcanics (Daly *et al.*, 1998; Stewart and Foden, 2001).

Quartz and feldspar phenocrysts, dacite clasts, amygdales and vitric shards are present throughout many of the suites and provide evidence of ash and lava flows that occurred throughout their formation (Rankin and Flint, 1991). The most extensive member of the Gawler Range Volcanics is the Yardea Dacite, which is located across almost half of the vicinity of the Gawler Ranges (Giles, 1988; Blisset, 1975).

Within the Nuyts Domain near Streaky Bay and to the east toward the Gawler Range Volcanic province is an interpreted complex of mafic/ultramafic bodies, largely under cover, and interpreted through magnetic data. These bodies have been drill cored in two locations by PIRSA, two holes drilled near the coast and three inland, at Corvisart Bay and Chandada respectively (Fig. 3), but attempted age-dating through SHRIMP zircon work has been unsuccessful (Ferris, pers comm.). The units are informally termed the Inkster Complex (Ferris, 2002). It is equally likely they may be related to the ca 1630 St. Peter arc-related magmatism or the ca 1580 Ma Hiltaba event magmatism. Such a distinction is critical in light of interpretations of exploration that target mafic Hiltaba related magmatism as a potential magmatic Ni-sulphide exploration target (e.g., WMC, Mithril Resources).

Regolith

Tertiary and Quaternary sediments extensively cover the crystalline basement of the Gawler Craton (Rankin and Flint, 1991). Palaeochannel systems, such as the Narlaby Palaeochannel and a smaller unnamed palaeochannel in the north and south-east of Streaky Bay respectively, can accommodate up to 100 m of Middle to Late Eocene Pidinga Formation and Pliocene Garford Formation sediments (Rankin and Flint, 1991) (Fig. 4). The Tertiary and Quaternary regolith has been described by Rankin and Flint (1991) and Parker (1993b) and their work is summarised below.

The sediments of the regolith profile near Streaky Bay are shown in Fig. 5. The Pidinga Formation consists of fine-grained to gravely, subangular to rounded sands and silts that are typically reduced or oxidised due to an intensely weathered environment. Interbeds of cream-grey and black carbonaceous clays are well developed within the formation, as is the presence of humic material and lignite (Fig. 5). Quartz is the major constituent of the sand, with other minerals such as pyrite, zircon and rutile in very small quantities. The sediments of the Pidinga Formation reflect periods of transgression and regression and indicate the possibility of the palaeochannel systems being part of an upper delta regime (Rankin and Flint, 1991).

Unconformably overlying the Pidinga Formation is the Garford Formation, a unit of fine to coarse-grained, angular to well-rounded silty sand. The sediments vary in colour from orange – pale yellow, red and purple. Similar to the Pidinga Formation, silty and carbonaceous clays occur throughout the Garford Formation, displaying shades of khaki to grey-green, brown and black (Fig. 5). Weathered basement and reworked Pidinga Formation sediments are the main contributors to the Garford Formation. Deposition of the sediments occurred in fluvial and lacustrine environments across the Gawler Craton (Rankin and Flint, 1991).

Ferricrete horizons are generally associated with the Pidinga and Garford Formations (Rankin and Flint, 1991). A nodular, mottled and pisolitic ferricrete has been developed within the Garford Formation and typically forms a cap over the Pidinga Formation. Another unit of ferruginous mottling and ferricrete occurs as horizons throughout the sand and silt of both formations. Silcrete layers are also present within both formations (Rankin and Flint, 1991).

Calcareous aeolinites and silts of the Middle to Late Pleistocene Bridgewater Formation unconformably cap the Tertiary formations and the Archean to Mesoproterozic crystalline basement (Rankin and Flint, 1991). The Bridgewater Formation occurs extensively over the Gawler Craton, including Streaky Bay (Fig. 3). The fine to medium-grained calcareous sediments were deposited in a coastal and inland dune system during times of frequent transgression and regression. A high-energy littoral and aeolian depositional environment of coastal sands is evident with the occurrence of irregular hummocky dunes. The coastal sediments were reworked as they were blown inland and have created oolitic calcrete in areas (Rankin and Flint, 1991). Bridgewater Formation cliffs surrounding the bay are up to 60 m high (Daniel, 2000). Inland the maximum thickness of the calcareous sediments is approximately 12 m.

3. Previous Exploration

Since 1966 areas around Streaky Bay have been explored for various commodities such as oil, gypsum, kaolin, uranium, coal and heavy-mineral sands. Very few companies have dedicated an exploration program exclusively to base and precious metals.

Western Mining Corporation Limited completed an exploration program for copper-gold mineralisation between 1992 and 1994. Compilation and assessment of open file data, geological mapping and numerous geophysical techniques such as gravity, magnetics, airborne radiometrics, TEM and IP were used initially to delineate specific target areas (WMC, 1994).

Subsequent drilling of 15 reverse circulation holes totalling 1006 m were drilled in the Wurkagie area. Within the 15 holes, ultramafic, mafic and felsic basement lithologies were intersected. Geochemistry, petrography and XRD analysis were performed to determine mineral composition of rock types and selected elemental abundances of samples throughout every hole (WMC, 1995).

CRA Exploration Pty Ltd (Env. 2127, 1972; Env. 4049, 1980-1982) spent some time exploring the possibility of uranium mineralisation in the Gawler Craton, especially in the west near Streaky Bay. Airborne radiometric surveys, electrical geophysics and percussion drilling were used to investigate the potential of mineralisation within the Hiltaba Suite granites and Tertiary sandstones. No significant results for uranium or any other base metals were detected when assayed. The best results were 10-18 ppm U, 20-50 ppm Pb, 145 ppm Cu and 95-106 ppm Zn (Rankin and Flint, 1991).

Western Nuclear Australia Ltd and partners Oilmin NL, Petromin NL and Transmin NL (Env. 5146, 1984) drilled 6 percussion holes at Karcultaby and Yandra, located east of Streaky Bay. (WMC, 1994, 1995). The locations of recent and previous mineral exploration licences are shown in Fig. 6.

4. Analytical Methods

In February 2003, Mithril Resources Limited completed a RAB drilling program, which consisted of 53 holes located east and north-east of Streaky Bay. Every hole was bagged and sampled at two metre intervals during drilling. Amdel Limited, Adelaide, performed analysis for economic elements for portions of the two-metre samples using the scheme IC2E.

The elements sampled and their detection limits were Ag (0.5 ppm), As (1 ppm), Bi (5 ppm), Cd (1 ppm), Co (1 ppm), Cr (2 ppm), Cu (1 ppm), Fe (100 ppm) Mn (5 ppm), Mo (1 ppm), Ni (1 ppm), Pb (3 ppm), P (5 ppm), Sb (5 ppm), V (1 ppm), Zn (1 ppm) and S (200 ppm). The scheme uses Inductively Coupled Plasma Optical Emission Spectroscopy (ICP-OES) for element analysis. Before the samples are analysed they require certain preparation, especially if solid. 1 ml of HNO_3 is added to a very small amount of sample (~ 0.5 g), which is then heated (at 215° C) for 30 minutes to allow the sediment to dissolve. After cooling 2.5 ml of HCl is added to the mix. The blend is then re-heated for 2 hours. Finally 11.7 ml of distilled water is added and the sample can be analysed by ICP-OES.

Further trace and economic element analysis was completed on selected samples of calcrete. The element abundances in this analysis were determined using the IC3E/M scheme, which employs both ICP-OES and ICP-MS (Inductively Coupled Plasma Mass Spectroscopy) methods. The preparation for this analysis required ~ 0.2 g of sediment to be mixed with 5 ml HCl, 3 ml HNO_3, 4 ml HF and 2 ml of $HClO_4$. The sample/acid blend is left for 4 hours and then heated (~300° C) for a further 4 hours. After cooling 5 ml of 6M ("50%") HCl is added and the sample is re-heated for 10 minutes. The addition of 15 ml of distilled water and 2 drops of H_2O_2 are the final requirements to prepare the sample entirely so it is ready to be presented to either ICP-OES or ICP-MS for analysis.

A simple experiment to determine the percentage of carbonate within the calcrete was completed at the University of Adelaide. Arbitrary amounts of sample (around 3 to 6 g) were weighed, placed in a beaker and covered with a 30% hydrochloric acid solution. The samples were left overnight to dissolve.

The remaining sediments were then filtered, rinsed and re-weighed. Weight differences were recorded and used to determine the amount of carbonate versus detrital material.

5. Geochemical Results

Basement Analysis

Major and trace element bivariate plots were used to compare the geochemical characteristics of mafic components of known Gawler Range Volcanic and comagmatic St. Peter Suite mafic phases with the mafic/ultramafic bodies intersected by the RR and CR drill holes in the Corvisart Bay and Chandada areas. Data sets used, include mafic Gawler Range Volcanics (Stewart, 1992), the mafic coastal outcrops of St. Peter Suite (Ferris, 2002) and drilled mafic/ultramafic Inkster Complex units of unknown age and origin (Ferris, 2002; WMC, 1995) (data sets are displayed in Table A–D, Appendix A). The location of the SADME drill holes is shown in Fig. 3. The purpose of the exercise was to delineate a possible association between the mafic/ultramafic Inkster Complex rocks and either the St. Peter Suite or the Gawler Range Volcanic event.

An assortment of variation graphs were produced using SiO_2 (%), Mg # and varied major oxide percentages along the X-axis. A minor selection of major element bivariate diagrams for SiO_2 (%) and Mg # along the x-axis are shown in Figs. 7a-h and 8a-i, respectively.

Major Elements

Harker diagrams of the Gawler Range Volcanics display coherent linear relationships between SiO_2 and major oxides. St. Peter Suite samples display random relationships for most elements in Harker diagrams and Mg # graphs. The SADME drill holes and rock samples and the WMC drill hole samples exhibit reasonably linear trends in the Harker diagrams and Mg # charts. In general TiO_2, Al_2O_3, K_2O and Na_2O increase and Fe_2O_3, MnO, MgO and CaO decrease with increasing SiO_2. For the Mg # plots most elements decrease, apart from an increase in CaO and MgO and random plots of P_2O_5 and Na_2O.

Trace Element

Trace element variation of SADME samples correlated with the St. Peter Suite and Gawler Range Volcanic samples is illustrated as spidergrams Figs. 9a and b.

CR and RR plots tend to display similar patterns. CR exhibits more variability in data and notable depletion and enrichment of Zr and Ba, respectively.

The SADME and Gawler Range Volcanic samples (Fig. 9a) exhibit comparatively similar REE patterns, although the Gawler Range Volcanic element abundances tend to be elevated.

A common shallow decreasing trend is observed between the three units in Fig. 9b. The St. Peter Suite data is variable and demonstrates differing element enrichments and depletions (Ba, Nb, Sr and Zr increase and U, Ce and Nd decrease for some samples, where the reverse is true for others). The CR and RR plots are generally confined within the boundaries of the range of the St. Peter Suite data, excluding a significant peak in Ba and decrease in Nb for the CR samples.

Regolith analysis

For the purpose of the investigation, the regolith profile was roughly divided into four units. The hard calcareous surface cover of Bridgewater Formation provides the basis for the first and most distinct component. Immediately beneath the calcrete layer, ferricrete or oxidised sands, silts and clays typically occur. This iron-rich region forms the second member. The third zone is represented by relatively clean medium-grained to gravely silts and sands that are both consolidated and unconsolidated. The second and third members correspond to sediments of the Garford and Pidinga Formations. The fourth zone is classed as the basement, which includes fresh sediments and clays that exhibit any relict igneous textures. The sediments, their typical depths and the thickness of the specific horizons are outlined in Fig. 10.

Transition Metals

Data of selected base metals including Ni, Cr, Mn, Fe and V were plotted against depth (Fig. 11a-h). These elements were chosen, as they are associated with mafic rocks and will be the best indicator elements for discriminating between mafic and felsic basements. Depth plots using WMC data were constructed to increase the understanding of base metal behaviour through the depth profile of the region (Fig. 12a-d). Ultramafic units are also intersected within some of the WMC drill holes, which present an opportunity to examine how metal behaviour varies above felsic and mafic bedrock lithologies. The depth plots also display element distributions throughout the profile of the drill holes, highlighting features within the lithological units from the surface to depth (Fig. 13a and b).

The most prominent feature identified, was a rapid increase of values observed at the base of the calcrete or a few metres below, usually within the ferruginous zone.

The transition ratio graphs provide information on element behaviour, variability and their associations with each other. Mithril drill hole samples with either mafic or felsic basements were selected to evaluate the possibility of identifying basement composition at the shallowest depth possible.

The data were separated approximately into the four profile zones and graphs were constructed for Cr, Cu, Fe, Ni, V and Zn versus Mn. Each chart in each division showed a variation of values corresponding to samples from either mafic or felsic units. The ranges of data for felsic and mafic units are listed in Table 1 and Fig. 14a-d shows Ni (ppm) graphs of the four zones before and after scaling.

Fig. 15a-d displays the change of Fe (ppm) abundances throughout the four zones. There tends to be Fe enrichment within the basement and ferruginous zones, whereas the sand and calcrete zones tend to be depleted.

Transition metal plots of Mithril and WMC drill hole data normalised to chondritic values are shown in Fig. 16a and b. Values on the graphs are representatives of element abundances of samples near surface (0 – 2 m depth) that overlie different basement lithologies. The Mithril samples data show large variation in elemental abundances. For many elements the highest and lowest values are represented by similar rock types, for example, Mn and Fe, Co and Ni for mafic and felsic units respectively.

Results from the WMC survey, demonstrate distinct patterns between lithology for many of the elements. Cr, Mn and in particular Ni illustrate this best, especially between felsic and ultramafic units.

Second sets of chondrite-normalised plots were produced for the same Mithril and WMC holes above (Fig. 17a and b). Values were selected from particular depth intervals that represented the start of the ferruginous zone for each hole. The pattern does not change significantly for the Mithril data, however an increase in V, Fe and Cu is evident for the mafic units.

The ultramafic data of the WMC plot alters noticeably as the pattern tends to flatten and Cr, Mn, Co and Ni values increase.

Dispersion plots of selected transition metals (Fig.18a-f) display the distribution of elements within the upper section of the ferruginous zone throughout the drill hole area. Regions of increased element abundance correspond for each plot.

Calcrete Analysis

Further comprehensive analysis, on selected calcrete samples (0 – 8 m depth) from Mithril drill holes were obtained from Amdel Ltd. Chondrite-normalised rare earth element (REE) diagrams of samples from 0 – 2 m, 2 – 4 m and 4 – 6 m depth intervals are similar to each other (Fig. 19a-c). All units exhibit a shallow decreasing trend with no significant enrichment or depletion of any element.

Six of the surface samples were treated with a 30% hydrochloric acid solution to remove any carbonate to allow for an apparent examination of the remaining detrital components. The residual material of the calcrete was rounded to angular, fine-grained quartz with some iron-oxide staining evident. Fine, dark red grains formed a very small percentage of the sediment. Weights and carbonate percentages are shown in Table 2.

6. Discussion

Basement distinctions

The mafic rock suites represented show varying degrees of correlation between major elements (Fig. 7a-h and 8a-j). There is no obvious discrimination between the RR and CR drill hole samples and the St Peter or the Gawler Range Volcanic samples, and it is difficult to assert from the major element data that the drilled mafic bodies are associated with either St Peter or Gawler Range lithologies. Assemblages of phenocrysts within the St. Peter Suite granitoids may create the variation of data displayed in the graphs (Rollinson, 1993).

The trace element spidergrams do allow some discrimination of the rock sample sets (Fig. 9a and b). The RR samples and the St Peter Suite samples exhibit similar trace element patterns in the primordial mantle-normalised trace element diagrams. The RR drill holes are located near the coast, close to outcropping St. Peter Suite, so it is quite reasonable to suggest that these are related. The CR drill holes are situated further inland. They share a much greater Nb-depletion and Ba-enrichment with the Gawler Range Volcanic samples. Absolute age data are difficult and expensive to acquire from mafic/ultramafic rocks. The suggestion here that the trace element characteristics may be useful in correlating the Inkster ultramafic bodies to either St Peter or Gawler Range Volcanics should be further tested with additional data.

Lithological regolith profiling

The extensive cover across the majority of Australia means that geochemical investigations of the regolith have become an increasingly popular method of exploration for concealed mineral deposits. Scott (1998), Lintern *et al.* (1998) and Scott and Martinez (1998) have studied the effects of weathering on various elements associated with gold and base metal mineral deposits throughout Australia. The initial requirement for any regolith research is to acquire an understanding of the entire profile including information regarding the landscape evolution and extent of weathering (Anand *et al.*, 2002).

The sediments that generate the regolith profile of the Streaky Bay region were described previously within the geological setting section of this paper. Additional assessment of the regolith reveals that its form is similar, although not identical to a typical laterite-saprolite profile (Aleva, 1994) (Fig. 20). The Bridgewater Formation calcrete and soil cover forms the present surface. The calcrete morphology is predominantly hardpan and has formed due to replacive and displacive accumulation of micritic carbonate, forming a massive, cemented layer (Chen *et al.*, 2002). Nodular and pisolitic structures are well developed, resulting from the dissolution and precipitation of the micritic carbonate (Chen *et al.*, 2002) or replacement of clays or nodular and pisolitic Fe-oxides by calcite and dolomite (Anand *et al.*, 1997). The base of the calcrete forms the surficial weathering front and is the beginning of the ferruginous zone, which consists of complex, nodular and pisolitic ferricretes (Bourman *et al.*, 1987) and mottled Fe-rich sediments.

The sediments beneath the ferruginous profile tend to vary throughout the region and include weathered basement clays, highly altered sediments and consolidated and unconsolidated sands. Previously this horizon was described as the sand zone, however, a more suitable classification would be the plasmic zone. This is a region of active mechanical, chemical and biological weathering that occurs rapidly after the deposition of sediments. An assortment of mineral assemblages assimilating with the interstitial pore fluids creates new minerals, typically various clays that have omitted any primary fabric (Aleva, 1994). Goethite and smectite are minerals formed within this zone and are associated with Cu and Ni respectively (Smith, 1977).

The base of the saprolite (weathered basement clays) forms the lower weathering front and the base of the regolith.

Geochemical regolith profiling

The depth plots display element distributions throughout the profile, which generally highlights the specific horizons (Fig. 11a-h). The most identifiable zone is the ferruginous profile, which displays elevated element concentrations. The calcrete exhibits no identifiable characteristics of element behaviour, which is also typical for the plasmic zone as well, except for a few increases in element values.

The variation of elemental concentrations is generated from the processes involved with the formation of the laterite-saprolite type profile present within the Streaky Bay region. Weathering of the crystalline basement produced secondary minerals generally associated with clay group minerals (Kronberg and Melfi, 1987). Deposition of the Pidinga and Garford Formations occurred during a temperate and wet climate (Rankin and Flint, 1991).

As a result of elevated water levels, the rate of geochemical dispersion of soluble elements such as Fe, Al and possibly Ni and Mn (Aleva, 1994) transpired from the weathered clays and through the porous sediments of the Tertiary formations.

The calcrete is the most recent sediment deposited and has been transported inland from various locations, such as marine settings (Daniel, 2000). Elemental depletion within the calcrete may be the consequence of various processes: 1) element dispersion throughout a regolith profile is regulated by time (Radford and Burton, 1999), which suggests that the Bridgewater Formation may be too young to have experienced sufficient element dispersion to display any geochemical signatures; 2) the calcareous layer is often hard and well cemented, which may restrict the movement of elements into the zone; 3) the process of element dispersion is commonly increased with the contribution of water (Rollinson, 1993; Butt *et al.*,1998). The calcareous sediments were deposited on the surface in relatively arid conditions (Rankin and Flint, 1991), which may indicate limited water and constrained movement of elements into the calcrete layer; and 4) the ferruginous zone may act as a trap and reservoir for the elements, restricting any element movement from the region.

The transition metal ratio plots proved to be the best indicator of rock type unit (Fig. 14a-d). The ranges of values for mafic and felsic holes displayed that there were often distinct differences in the data for the different units (Table 1). For the majority of elements the highest values were displayed for units of mafic lithologies. Within the lateritic profile, where element abundances were most elevated, basement rock type determination could be decided, relatively confidently.

Simple leaching of the calcrete exposed detrital material consisting of sub-angular to rounded, fine-grained quartz and 1-2% fine-grained opaque minerals.

In some samples small clasts of quartz and opaque grains tightly compacted with carbonate remained, which illustrates the extent of cementation of the calcrete. Up to 75% of carbonate is present in the calcrete. It is possible that the detrital component of the Bridgewater Formation reflects fragments derived from *in situ* weathering of the basement, and incorporated within the aeolian Bridgewater Formation carbonate material. The element dispersion plots (Fig. 18a-f) display the zones of element enrichment within the drill hole region near Streaky Bay. The element dispersion halo is generally larger than the region of enrichment (Smith, 1977), however, the diagrams are indicative of regions that show enrichment and could be explored in more detail.

7. Conclusions

The basement analysis results are inconclusive for both the major element data. An association of the mafic units from the CR and RR drill holes with the St. Peter Suite and the Gawler Range Volcanics respectively is suggested by the trace element data. Future investigations of the ambiguous mafic units should involve the compilation of a wider data set and comparisons with more specific data, such as with known Hiltaba Suite or St. Peter Suite age samples collected from locations near the holes. Dating the age of the CR and RR samples would also be important if achievable.

The most significant conclusion to arise from this study were the results attained from the transition metal depth plots and ratio graphs. Element dispersion patterns were clearly demonstrated for both, and the location of the enriched ferruginous layer was identified for all drill holes in this study.

The element concentration ranges determined from the ratio plots can be utilized to determine the basement lithology from depths around 6 – 14 m, at the commencement of the enriched horizon.

Values in excess of the maximum ranges of elements established for felsic lithologies indicate a mafic basement. For the majority of elements the maximum mafic basement values greatly exceed felsic basement values, especially Fe, Cu and Zn and basement rock type can be identified for most samples.

Study of the calcrete proved that the utility of trace elements in distinguishing basement lithology at or near surface is unreliable in this region. This suggests that relatively expensive drilling would still be a part of any exploration program. The total depth of the drill holes, however, is substantially decreased, due to the demonstrated link between basement lithology and ferruginous horizons. The dispersion graphs would be a useful tool in exploration as they highlight regions of exploration significance and indicate areas creditable for supplementary exploration.

8. Acknowledgements

I would like to start by thanking Karin Barovich for her continuous support. Karin allowed me to work independently throughout the year, although was always on hand when I required any extra help. Through her extensive knowledge of geochemistry I found I was motivated to work in an area of geology in which I have never before been involved with.

I would also like to thank the Cooperative Research Centre for Landscape Evolution and Mineral Exploration (CRC LEME) for the scholarship money they provided, which allowed me to devote full time this year to my project.

Jim, David and Barry from Mithril Resources were always there when I needed inspiration, support and an insight into the industrial aspects of mineral exploration. Thanks also for their invaluable assistance for making their data available to me for this study. I would also like to thank Ian Morgan, the owner of Yandra Station, for showing me the Mithril drill hole locations during a visit to Streaky Bay.

Last, but not least, I express so much appreciation to Mum, Dad, Sarah and Indi for their continuous support throughout the year, in good times and bad.

APPENDIX A

MAJOR AND TRACE ELEMENT DATA SETS

Table A. Gawler Range Volcanics data set (From Stewart, 1992)

Sample:	K101	884-K8	K33	K110	884-K3	884-K5	K122	884-K28	K153	884-GH1	884-GH2	E231
Unit:	LPT Basalt	LPT Basalt	LPT Basalt	LPT Basalt	HPT Basalt	HPT Basaltic Andesite	HPT Basaltic Andesite	HPT Basaltic Andesite	IPT Basaltic Andesite	Nukalla Basalt	Nukalla Basalt	Nukalla Basalt
SiO2	51.91	51	52.01	51.94	52.96	54.22	54.28	53.49	53.69	50.85	50.65	50.85
TiO2	0.64	0.62	0.82	0.85	2.21	2.04	2.32	2.18	1.74	1.17	1.15	1.15
Al2O3	13.65	14.14	16.02	15.87	14.23	14.07	14.62	14.25	14.81	17.13	17.01	16.71
Fe2O3	9.66	9.62	10.79	10.18	12.07	13.47	12.02	12.12	13.57	10.18	10.15	10.22
FeO												
MnO	0.18	0.17	0.19	0.18	0.25	0.18	0.23	0.22	0.21	0.18	0.18	0.16
MgO	11.77	10.96	8.44	7.72	3.28	2.41	3.27	3.39	3.53	4.68	5.45	5.45
CaO	8.55	7.54	8.62	8.88	7.05	5.14	6.57	6.63	6.54	7.78	7.8	6.4
Na2O	2.15	3.15	2.51	2.59	2.7	2.69	3.01	2.76	3.23	3.14	3.56	3.7
K2O	1.27	0.28	1.06	1.23	3.14	3.51	2.75	2.51	2.2	2.46	1.71	2.33
P2O5	0.18	0.18	0.25	0.24	1.33	0.82	1.07	1.37	0.4	0.22	0.22	0.21
LOI	1.51	1.97	1.46	2.12	0.53	1.21	0.8	0.65	0.7	2.03	2.23	2.52
Mg #	54.92	53.26	43.89	43.13	21.37	15.18	21.39	21.86	20.64	31.49	34.94	34.78
Ba	1005	492	718	842	2135	2456	1700	1377.9	976	781	482	695
Rb	45	9.7	36	42	72	69	82	117.9	67	99	56	85
Th		5.7			9.4	11		10.4		6.2	6.2	
U		2.8			6	3.5		2.6		0.3	3.6	
Nb	5.3	4.8	5.9	5.6	9.6	8.8	11	10.1	9.5	8.5	8.9	8.6
La		27			57	44		62		27	28	
Ce	78	66	58	54	133	108	120	129.3	86	60	63	52
Sr	510	427	480	547	635	529	519	552.6	433	401	450	529
Nd	36	32		21	66	41	63	65.9	45	27	35	25
Sm												
Zr	102	102	124	119	233	220	234	230.8	229	163	162	159
Y	19	19.7	23	24	51	45	52	49.9	40	28	28	28
Ni		289	192	197	5	6	8.4	2.2	8.4	96	93	112
Cu												
Pb		12			15	12		10.8		12	9	
V		182	176	179		217	167	129.7	280	203	198	188
Cr		941	600	619		5	14	0	8.1	63	61	106
Zn												

Table B. St. Peter Suite data set (from Ferris, 2002)

Sample No.:	R434792	GDRP8	MDPJ8	R432666	R434657	R434659	R432678	R434661	R434662	R434663	R432688	R432693	R432698	R434669	R432710	R432721
Unit:	ST PETER	ST PETER	ST PETER	ST PETER	ST PETER	ST PETER	ST PETER	ST PETER	ST PETER	ST PETER	ST PETER	ST PETER	ST PETER	ST PETER	ST PETER	ST PETER
Group:	2	2	2	mafic	mafic	mafic	mafic	mafic	mafic	mafic	mafic	mafic	mafic	mafic	mafic	mafic
SiO2	56.4	57.4	57.49	46.7	41.4	44.4	56.25	51	47.6	42.9	51.72	52.53	53.17	45.9	50.39	48.52
TiO2	0.775	0.99	0.84	1.06	1.28	1.27	1.36	1.59	1.77	0.2	2.03	0.08	0.51	0.255	0.66	1.2
Al2O3	16.8	15.77	17.77	21.31	19.9	18.4	18.43	16.6	16.6	16.7	33.97	42.65	22.32	24.8	19.38	20.89
Fe2O3	8.9	9.8	7.43	14.96	13.7	13.9	10.33	11.3	12	10.2	8.84	1.77	9.8	5.72	12.7	13.82
MnO	0.12	0.23	0.15	0.1	0.17	0.16	0.12	0.17	0.16	0.14	0.01	0.01	0.22	0.09	0.13	0.37
MgO	3.88	3.19	2.95	1.85	4.87	4.36	3.38	4.64	5.28	16.5	0.09	0.23	5.13	4.62	8.04	4.15
CaO	6.4	6.46	6.28	9.34	14	14.1	4.81	7.18	8.62	9.15	0.02	0.61	4.99	13.7	7.87	6.32
Na2O	3.63	4.71	3.92	2.73	1.3	0.79	2.79	2.85	2.83	1.04	0.55	0.7	2.1	1.5	0.92	2.8
K2O	2.14	0.77	1.61	0.98	0.87	0.56	1.91	2.19	2.14	0.5	0.91	0.25	1.27	1.09	0.33	1.37
P2O5	0.2	0.46	0.44	0.12	0.03	0.04	0.94	1.23	1.37	0.08	0.12	0.01	0.04	0.03	0.03	0.17
LOI		0.46	0.92													
Mg #	30.36	24.56	28.42	11.01	26.23	23.88	24.65	29.11	30.56	61.80	1.01	11.50	34.36	44.68	38.77	23.09
Ba	750	315	1159	310	300	175	700	800	750	190	260	90	330	350	110	440
Rb	67	17.5	48.7	160	56	30	165	98	68	16.5	17.5	9	61	42	28	73
Th	10.5	2	3.9	4.2	1.15	1.4	10.5	12.5	6.5	1.65	10	0.76	1.75	2.1	2.8	1.65
U	2.6	-0.3	0.3	3.9	0.25	0.58	3.8	2.6	1.65	0.29	3.1	1.8	1.7	0.21	0.82	0.27
Nb	15	11.6	3	5	5	5	5	10	10	5	5	5	5	5	5	5
La	26	22	23	13	4	5.5	44	37.5	32	7	43.5	1.8	25	6.5	23.5	16
Ce	39.5	75	53	20.5	8.5	11.5	81	61	54	12.5	125	3	40	6.5	64	34
Sr	500	468.9	994.1	550	490	450	600	480	500	480	105	50	300	600	185	750
Nd	32	42	25	13	7	10.5	43.5	60	58	9	17	1.3	29	8	36.5	25.5
Sm	4.6			3.3	1.35	1.95	10	10	10	1.35	3.2	0.33	7.5	1.35	8.5	6
Zr	100	175.1	121.2	60	60	50	90	100	100	50	230	60	50	20	60	120
Y	25	53.7	19.5	27.5	10	14.5	29.5	45	43.5	11.5	14.5	0.95	83	8.5	12	24
Ni	40	4	5	44	6	11	20	4	2	290	18	52	115	52	49	27
Cu	77	18	12	125	48.5	67	24	35	32	32	41	78	240	66	140	145
Pb	14.5	13.7	5.7	12.5	13.5	10	8.5	7.5	5.5	3	21.5	4.5	5.5	3.5	5	5
V	160	132	166	250	380	400	170	220	260	50	310	10	130	120	260	300
Cr	60	0.5	0.5	40	10	10	60	10	10	600	90	50	150	90	90	30
Zn	115	130	107	200	75	88	99	80	88	86	99	10.5	160	62	90	220

Table C. SADME CR and RR drill hole data set (from Ferris, 2002)

Sample No.:	R506797	R506798	R506799	R506800	R506802	R506803	R506804	R506805	R506806	R506807	R506817	R506818	R506819	R506820
Drill hole:	CR-3	CR-3	CR-3	RR-1	RR-1	RR-3	RR-3	CR-2	CR-2	CR-2	rock sample	rock sample	rock sample	rock sample
Depth of sample:	284.9-285.5ft	285.5-286.1f	287-288ft	312-313ft	320.3-321.1f	206.9-207.5ft	10.8-211.4f	250-250.11f	50.11-251.8f	252.3-253ft				
SiO2	46.91	47.05	45.41	48.35	47.98	50.68	52.03	47.95	49.20	47.55	44.08	44.70	45.45	45.56
TiO2	0.19	0.20	0.17	1.58	1.65	1.21	0.99	0.54	0.81	0.57	0.07	0.11	0.11	0.13
Al2O3	9.79	9.45	8.97	15.41	15.56	15.95	18.60	15.78	15.35	15.41	24.33	23.50	25.51	24.00
Fe2O3	19.06	19.49	19.62	15.81	15.76	13.61	9.96	12.57	12.10	12.88	6.54	6.35	4.85	5.68
MnO	0.51	0.37	0.35	0.18	0.18	0.19	0.15	0.22	0.21	0.24	0.10	0.10	0.08	0.09
MgO	18.16	18.03	20.39	5.97	5.86	6.65	5.43	12.67	11.79	12.98	10.60	10.65	6.46	7.58
CaO	3.76	3.80	3.84	9.40	9.79	7.95	8.41	7.50	7.07	7.80	12.79	13.16	16.40	15.86
Na2O	1.23	1.23	0.99	2.53	2.53	2.81	3.38	2.02	2.12	1.93	0.93	0.92	1.06	1.02
K2O	0.31	0.30	0.19	0.68	0.59	0.83	0.90	0.41	1.06	0.43	0.52	0.44	0.06	0.06
P2O5	0.08	0.08	0.08	0.08	0.11	0.11	0.14	0.34	0.28	0.22	0.05	0.05	0.03	0.02
LO1	9.98	9.38	8.78	0.73	0.86	1.92	2.13	1.25	1.97	1.34	4.08	3.64	1.51	1.7
Mg #	48.80	48.06	50.96	27.42	27.11	32.83	35.27	50.20	49.36	50.20	61.86	62.65	57.12	57.13
Ba	3150	5950	2100	420	370	470	440	430	850	390	100	185	195	95
Rb	11.5	10.5	8.5	17	14.5	18.5	22.5	8.5	33.5	9.5	1	17	16	1
Th	0.57	0.46	0.46	1.8	1.6	1.8	1.95	0.7	2.7	0.66	0.11	0.07	0.07	0.08
U	0.16	0.17	0.16	0.33	0.3	0.33	0.39	0.13	0.47	0.15	0.04	0.03	0.03	0.03
Nb	0.5	0.5	0.5	4	3.5	5.5	5	1.5	3	1.5	0.5	0.5	0.5	0.5
La	5.5	4.5	4.5	10.5	10	14	14	14	17.5	10	2.5	2	1	1.5
Ce	8.5	8.5	7.5	18.5	18	26	25.5	25.5	32.5	17.5	4	3.5	2	3
Sr	165	290	125	380	360	370	480	650	550	650	750	900	900	900
Nd	4.6	4.2	4.1	10.5	10.5	15.5	13.5	13	17	10	2	2.1	1.65	1.9
Sm	1.25	1.45	1.1	2.8	2.9	4	3.1	2.8	3.6	2.1	0.42	0.48	0.45	0.53
Zr	30	20	20	60	70	60	70	30	30	30	30	30	20	20
Y	4.7	4.2	4	15.5	15.5	19.5	15.5	9.5	12	8.5	1.2	1.55	1.65	2.1
Ni														
Cu	88	81	98	120	115	89	54	67	64	80	27.5	23	45.5	49.5
Pb	6.5	3.5	3.5	5.5	4.5	5.5	6	3	4.5	3	2	1.5	1.5	1
V	40	30	30	440	450	250	150	90	110	100	20	40	60	70
Cr	160	160	130	90	70	120	70	250	210	260	210	340	340	370
Zn	185	125	93	125	115	115	88	98	99	90	50	38.5	34.5	22

Table D. Ultramafic/mafic data set (From WMC, 1995)

Sample No.:	DA780545	DA780567	DA780570	DA780573	DA780574
Unit:	Peridotite	Peridotite	Peridotite	Gabbro	Gabbro
Drill Hole:	SBYC1	SBYC14	SBYC15	SBYC5	SBYC4
SiO2	40.5	38.4	37.4	47.5	49.1
TiO2	0.29	0.14	0.2	0.21	0.17
Al2O3	7.1	5.55	3.3	22.2	25.9
Fe2O3	13	12.8	14.1	4.65	2.85
FeO					
MnO					
MgO	24.3	29	32.5	6.95	4.06
CaO	3.74	2.42	1.41	10.3	11.5
Na2O	0.9	0.4	0.4	2.5	2.8
K2O	0.11	0.09	0.04	0.64	0.36
P2O5					
LOI	6.1	6.5	5.2	2.4	2.1
Mg #					
Ba	40	40	45	235	210
Rb					
Th					
U					
Nb	1	1	1	1	1
La					
Ce					
Sr					
Nd					
Sm					
Zr	5	5	5	5	5
Y	6	2	1	4	3
Ni	1300	1500	1800	235	105
Cu	85	40	35	40	50
Pb	2	2	2	4	4
V					
Cr	2000	1800	2950	475	310
Zn	120	110	100	40	20

9. References

Aleva, G.J.J. (compiler), 1994. Laterites. Concepts, geology, morphology and chemistry. ISRIC, Wageningen.

Anand, R.R., Phang, C., Wildman, J.E. and Lintern, M.J., 1997. Genesis of some calcretes in the southern Yilgarn Craton, Western Australia: Implications for mineral exploration. *Australian Journal of Earth Sciences.*, 44: 87-103.

Anand, R.R., Fraser, S.J., Jones, M.R., Shu, Li, Munday, T.J., Phang, C., Robertson, I.D.M., Scott, K.M., Vasconcelos, P., Wildman, J.E. and Wliford, J., 2002. Geochemical exploration in regolith-dominated terrain, North Queensland. Final Report of CRC LEME-AMIRA project P417, CRC LEME open file report 120.

Blisset, A.H., 1975. Rock units in the Gawler Range Volcanics. Q. Geol. Notes, Geol. Surv. South Aust., 55: 2-14.

Bourman, R.P., Milnes, A.R. and Oades, J.M., 1987. Investigations of ferricretes and related surficial ferruginous materials in parts of southern and eastern Australia. In: M.J., McFarlane, (editor), Laterites. Some aspects of current research. Gebruder Borntraeger, Berlin.

Butt, C.R.M, Gray, D.J., Lintern, M.J., Robertson, I.D.M., Taylor, G.F. and Scott, K.M., 1998. Gold and associated elements in the regolith-dispersion processes and implications for exploration. Final Report of CRC LEME project P241, CRC LEME open file report 29.

Chen, X.Y., Lintern, M.J. and Roach, I.C., 2002. Calcrete: Characteristics, distribution and use in mineral exploration. Instant Colour Press, Belconnen ACT.

Creaser, R.A., 1989. The geology and petrology of middle Proterozoic felsic magmatism of the Stuart Shelf, South Australia. Latrobe University. Ph.D. thesis (unpublished).

Daly, S.J., Fanning, C.M. and Fairclough, M.C. 1998. Tectonic evolution and implications for exploration potential of the western Gawler Craton. *AGSO Journal of Australian Geology and Geophysics*, 17, 145-168.

Daniel, R.F., 2000. Carbonate sediments of a cool-water embayment, Streaky Bay, South Australia: Lithofacies and controlling factors. Department of Geology and Geophysics, University of Adelaide. Ph.D. thesis (unpublished).

Ferris, G.M., 2002. The geology and geochemistry of granitoids in the Childara region, western Gawler Craton, South Australia: Implications for the Proterozoic tectonic history of the western Gawler Craton and the development of lode-style gold mineralisation at Tunkillia. University of Adelaide. MSc. Thesis (unpublished).

Ferris, G.M., Schwarz, M.P. and Heithersay, P. 2002 - The geological framework, distribution and controls of Fe-oxide Cu-Au mineralisation in the Gawler Craton, South Australia: Part I – geological and tectonic framework. In: T.M., Porter, (Editor), Hydrothermal Iron Oxide Copper-Gold & Related Deposits: A Global Perspective, Volume 2; PGC Publishing, Adelaide, pp 9 – 32.

Flint, R.B., 1993. Chapter 5: Mesoproterozoic. In: J. F., Drexel, W.V., Preiss and A. J., Parker (Editors). The geology of South Australia: Vol. 1 The Precambrian. South Australia. Geological Survey, Bulletin.

Friedrich, G.H.W and Christensen, S.M., 1977. Geochemical dispersion patterns associated with the Lake Yindarlgooda sulphide mineralization, Western Australia. *J. Geochem. Explor.*, 8, 219-234.

Giles, C.W., 1988. Petrogenesis of the Gawler Range Volcanics, South Australia. *Precambrian Res.*, 40/41: 407-427.

Kronberg, B.I and Melfi, A.J., 1987. The geochemical evolution of lateritic terranes. In: M.J., McFarlane, (editor), Laterites. Some aspects of current research. Gebruder Borntraeger, Berlin.

Lintern, M.J, Sheard, M.J. and Gray, D.J., 1998. Geochemical studies of the regolith at the Mt. Gunson copper deposits, Stuart Shelf, South Australia. CRC LEME restricted report 76R.

Parker, A.J., 1990. Gawler Craton and Stuart Shelf – regional geology and mineralisation. In: F.E., Hughes (Editor), Geology of the mineral deposits of Australia and Papua New Guinea. Australasian Institute of mining and Metallurgy. Monograph Series, 14:999-1008.

Parker, A.J. 1993a. Palaeoproterozoic. In: J. F., Drexel, W.V., Preiss and A. J., Parker (Editors). The geology of South Australia: Vol. 1 The Precambrian. South Australia. Geological Survey, Bulletin, 54:51-105.

Parker, A.J. 1993b. Palaeoproterozoic. In: J. F., Drexel and W.V., Preiss (Editors). The geology of South Australia: Vol. 2 The Phanerozoic. South Australia. Geological Survey, Bulletin.

Radford, N.W. and Burton, P.E., 1999. The geochemistry of transported overburden: The time factor. An example from the Fender deposit, Big Bell, Western Australia. *J. Geochem. Explor.*, 66: 71-83.

Rankin, L.R. & Flint, R.B. 1991. STREAKY BAY, South Australia Sheet SI 53-2. South Australia. Geological Survey. 1:250 000 Series – Explanatory Notes.

Rattigan, J.H., Gersteling, R.W. and Tonkin, D.G., 1977. Exploration geochemistry of the Stuart Shelf, South Australia. *J. Geochem. Explor.*, 8, 203-217.

Rollinson, H.R., 1993. Using geochemical data: Evaluation, presentation, interpretation. Longman Group UK Limited.

Scott, K.M., 1998. Mineralogy and geochemistry of weathered mafic/ultramafic volcanics from section 42000N at Panglo, eastern Goldfields, Western Australia. CRC LEME open file report 14.

Scott, K.M. and Martinez, A., 1998. The mineralogical and geochemical effects of weathering in mafic and ultramafic profiles, Mt. Magnet, Western Australia. CRC LEME open file report 30.

Smith, B.H., 1977. Some aspects of the use of geochemistry in the search for nickel sulphides in lateritic terrain in Western Australia. *J. Geochem. Explor.*, 8: 259-281.

Stewart, K.P., 1992. High temperature felsic volcanism and the role of mantle magmas in Proterozoic crustal growth in the Gawler Range Volcanic province. Department of Geology and Geophysics, University of Adelaide. Ph.D. thesis (unpublished).

Stewart, K.P and Foden, J., 2001. Mesoproterozoic granitoids of South Australia: Part 1 – the Gawler Craton. Department of Geology and Geophysics, University of Adelaide (unpublished).

Thomson, B.P., 1970. A review of the Precambrian and Lower Palaeozoic tectonics of South Australia. Transactions, 94:193-221.

Thomson , B.P., 1975. Gawler Craton, S.A. In: C.L., Knight (Editor), Economic Geology of Australia and Papua New Guinea, 1, Metals. Australian Institute of Mining and Metallurgy. Monograph Series, 5:461-466.

Twidale, C.R. and Campbell, E.M., 1993. Australian landforms: Structure, process and time. Gleneagles Publishing, Glen Osmond, South Australia.

WMC Ltd. 1994. EL 1811, Streaky Bay, S.A. Annual report from 8/12/92 to 7/12/93. South Australia. Department of Mines and Energy.

WMC Ltd. 1995. EL 1811, Streaky Bay, S.A. Annual report from 8/12/93 to 7/12/92. South Australia. Department of Mines and Energy.

Table 1. Element concentration ranges for samples from mafic and felsic basements separated into the four regolith zones

Basement Lithology:	Mafic				Felsic			
Zone:	Calcrete	Fe-rich	Sand	Basement	Calcrete	Fe-rich	Sand	Basement
Mn (ppm)	34 - 175	12 - 600	6 - 280	22 - 2850	24 - 200	18 - 210	8 - 64	14 - 330
Cr (ppm)	7 - 105	9 - 120	3 - 68	2 - 900	9 - 32	21 - 54	2 - 36	4 - 33
Cu (ppm)	6 - 29	4 - 350	1 - 120	2 - 270	4 - 32	6 - 23	1 - 17	1 - 98
Fe (ppm)	2050 - 160000	7300 - 235000	1450 - 65200	2950 - 215000	1900 - 37100	9100 - 105000	950 - 39900	3200 - 40900
Ni (ppm)	2 - 10	2 - 56	1 - 44	1 - 400	2 - 11	2 - 12	1 - 21	1 - 66
V (ppm)	7 - 460	12 - 750	1 - 185	19 - 320	4 - 100	15 - 140	4 - 49	10 - 30
Zn (ppm)	4 - 18	3 - 140	2 - 125	8 - 300	5 - 29	5 - 32	3 - 29	4 - 165

Table 2. Weights before and after leaching of selected calcrete samples.

			Orignal		After Leaching		
Hole Number	Sample Number	Weight of Tray (g)	Weight of Sampe + Tray (g)	Weight of Sample (g)	Weight of Sampe + Tray (g)	Weight of Sample (g)	% of Carbonate
SBAC-001	P430003	2.1	8.71	6.61	5.512	3.412	48.38
SBAC-003	P430054	2.1	10.125	8.025	6.883	4.783	40.4
SBAC-007	P430124	2.1	7.417	5.317	4.26	2.16	59.38
SBAC-015	P430258	2.1	8.551	6.451	5.651	3.551	44.95
SBAC-025	P430475	2.1	7.644	5.544	5.219	3.119	43.74
SBAC-026	P430497	2.1	7.962	5.862	3.592	1.492	74.55

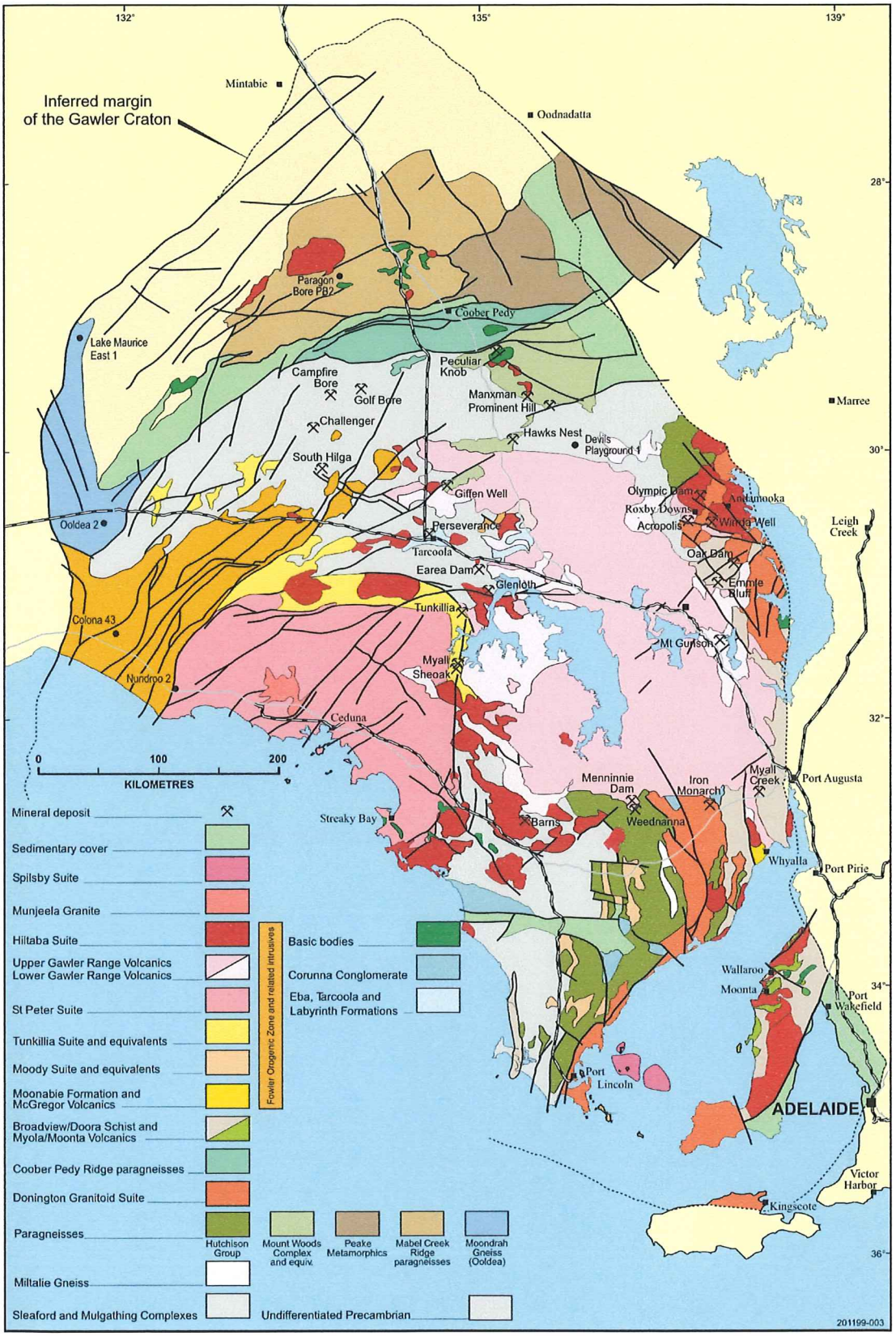
132°
135°
139°
28°
30°
32°
34°
36°
Inferred margin
of the Gawler Craton
Mintabie
Oodnadatta
Marree
Paragon
Bore PB2
Coober Pedy
Lake Maurice
East 1
Peculiar
Knob
Campfire
Bore
Golf Bore
Manxman
Prominent Hill
Challenger
Hawks Nest
Devils
Playground 1
South Hilga
Giffen Well
Olympic Dam
Roxby Downs
Acropolis
Andamooka
Wirrda Well
Leigh
Creek
Ooldea 2
Perseverance
Tarcoola
Oak Dam
Earea Dam
Glenloth
Emmie
Bluff
Tunkillia
Colona 43
Mt Gunson
Myall
Sheoak
Nundroo 2
Ceduna
0
100
200
KILOMETRES
Menninnie
Dam
Iron
Monarch
Myall
Creek
Port Augusta
Streaky Bay
Barns
Weednanna
Whyalla
Port Pirie
Wallaroo
Moonta
Port
Wakefield
Port
Lincoln
ADELAIDE
Victor
Harbor
Kingscote
Mineral deposit
Sedimentary cover
Spilsby Suite
Munjeela Granite
Hiltaba Suite
Upper Gawler Range Volcanics
Lower Gawler Range Volcanics
St Peter Suite
Tunkillia Suite and equivalents
Moody Suite and equivalents
Moonabie Formation and
McGregor Volcanics
Broadview/Doora Schist and
Myola/Moonta Volcanics
Coober Pedy Ridge paragneisses
Donington Granitoid Suite
Paragneisses
Hutchison
Group
Mount Woods
Complex
and equiv.
Peake
Metamorphics
Mabel Creek
Ridge
paragneisses
Moondrah
Gneiss
(Ooldea)
Miltalie Gneiss
Sleaford and Mulgathing Complexes
Undifferentiated Precambrian
Fowler Orogenic Zone and related intrusives
Basic bodies
Corunna Conglomerate
Eba, Tarcoola and
Labyrinth Formations
201199-003

Fig. 1.

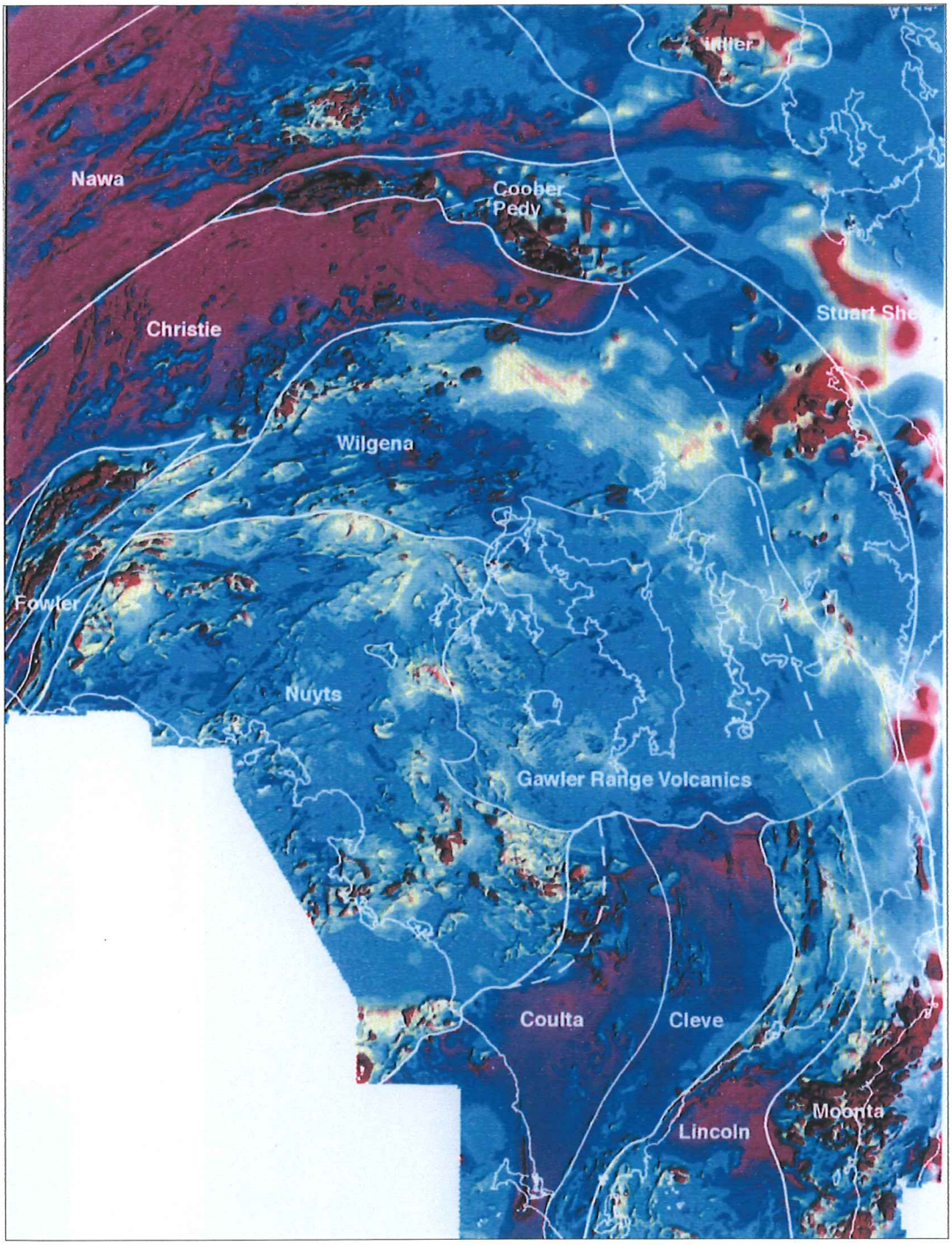
Nawa
Coober Pedy
Christie
Wilgena
Fowler
Nuyts
Gawler Range Volcanics
Coulta
Cleve
Lincoln
Mobrta

Fig. 2.

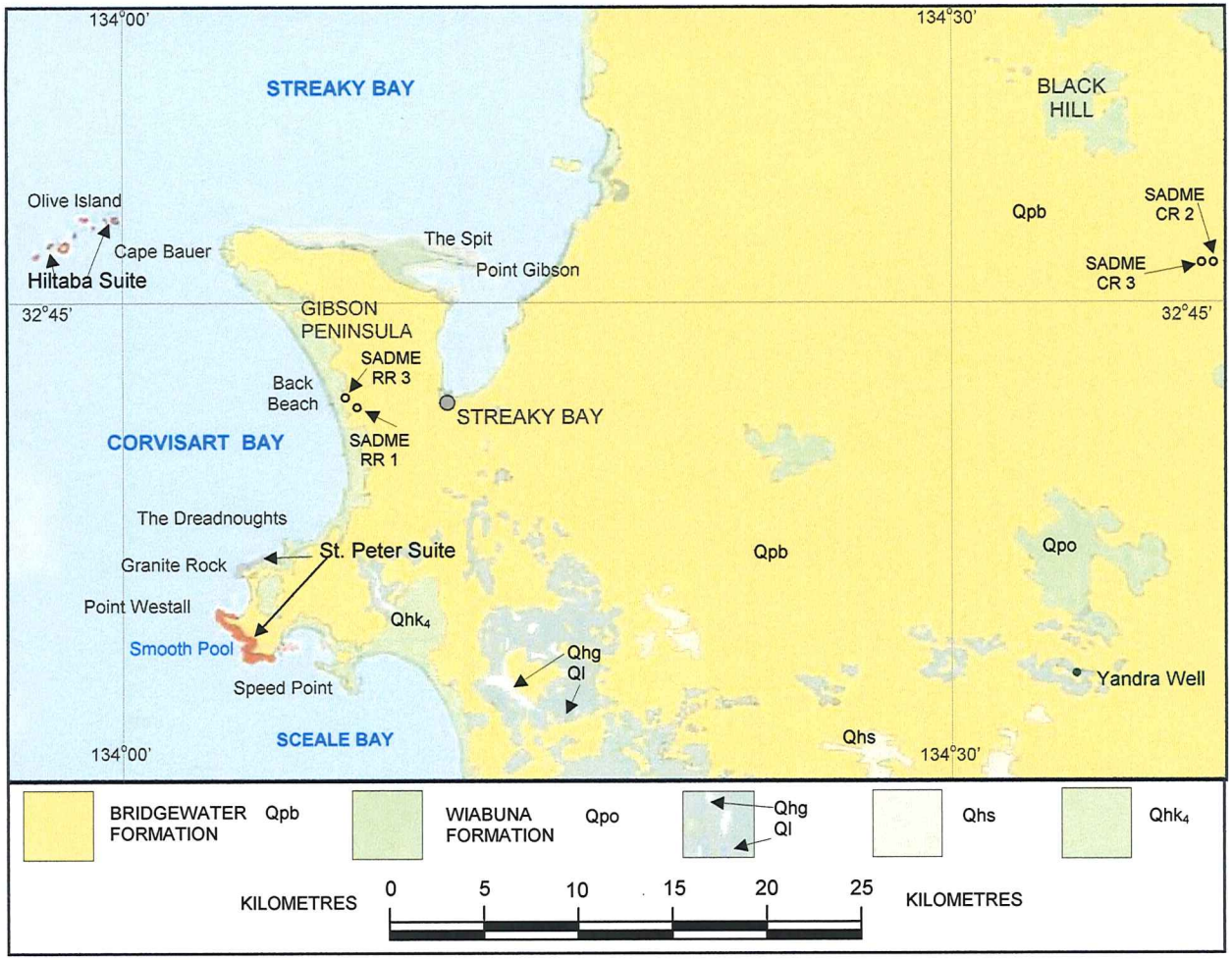
134°00'
134°30'
STREAKY BAY
BLACK HILL
Olive Island
Cape Bauer
Hiltaba Suite
The Spit
Point Gibson
Qpb
SADME CR 2
SADME CR 3
32°45'
GIBSON PENINSULA
SADME RR 3
Back Beach
STREAKY BAY
CORVISART BAY
SADME RR 1
The Dreadnoughts
Granite Rock
St. Peter Suite
Qpb
Qpo
Point Westall
Qhk4
Smooth Pool
Qhg
Ql
Yandra Well
Speed Point
SCEALE BAY
Qhs
134°00'
134°30'
BRIDGEWATER FORMATION Qpb
WIABUNA FORMATION Qpo
Qhg
Ql
Qhs
Qhk4
KILOMETRES
0 5 10 15 20 25
KILOMETRES

Fig. 3.

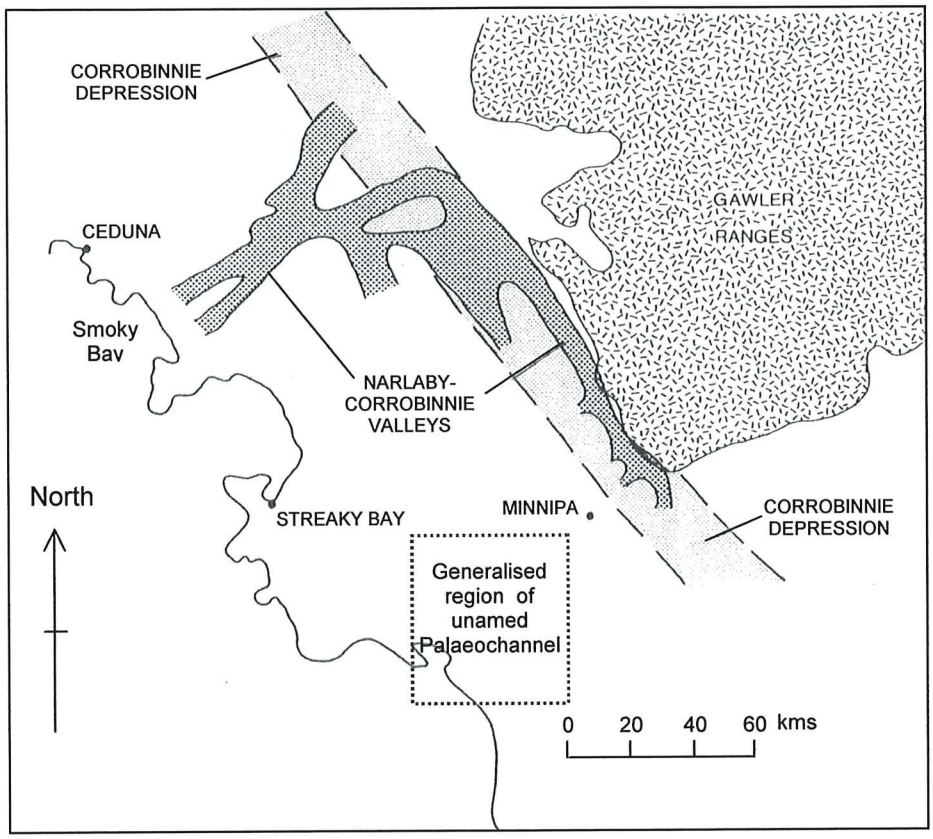
CORROBINNIE
DEPRESSION
CEDUNA
Smoky
Bav
GAWLER
RANGES
NARLABY-
CORROBINNIE
VALLEYS
North
STREAKY BAY
MINNIPA
CORROBINNIE
DEPRESSION
Generalised
region of
unamed
Palaeochannel
0 20 40 60 kms

Fig. 4.

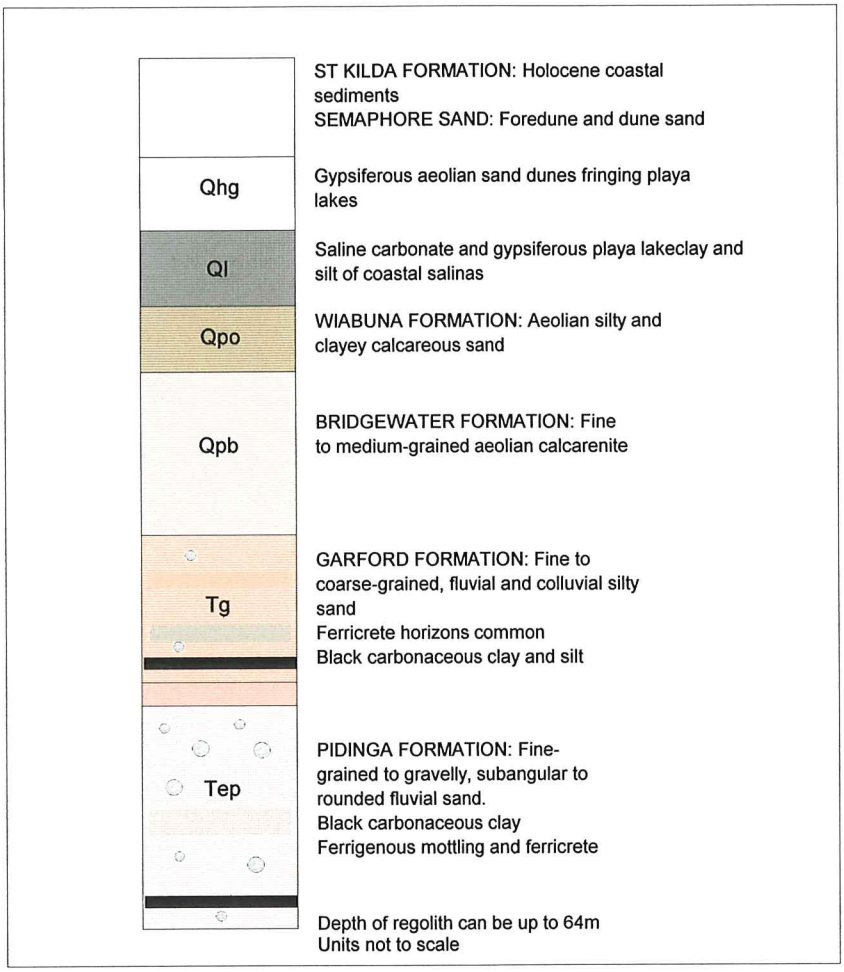
ST KILDA FORMATION: Holocene coastal sediments
SEMAPHORE SAND: Foredune and dune sand
Qhg
Gypsiferous aeolian sand dunes fringing playa lakes
Ql
Saline carbonate and gypsiferous playa lakeclay and silt of coastal salinas
Qpo
WIABUNA FORMATION: Aeolian silty and clayey calcareous sand
Qpb
BRIDGEWATER FORMATION: Fine to medium-grained aeolian calcarenite
Tg
GARFORD FORMATION: Fine to coarse-grained, fluvial and colluvial silty sand
Ferricrete horizons common
Black carbonaceous clay and silt
Tep
PIDINGA FORMATION: Fine-grained to gravelly, subangular to rounded fluvial sand.
Black carbonaceous clay
Ferrigenous mottling and ferricrete
Depth of regolith can be up to 64m
Units not to scale

Fig. 5.

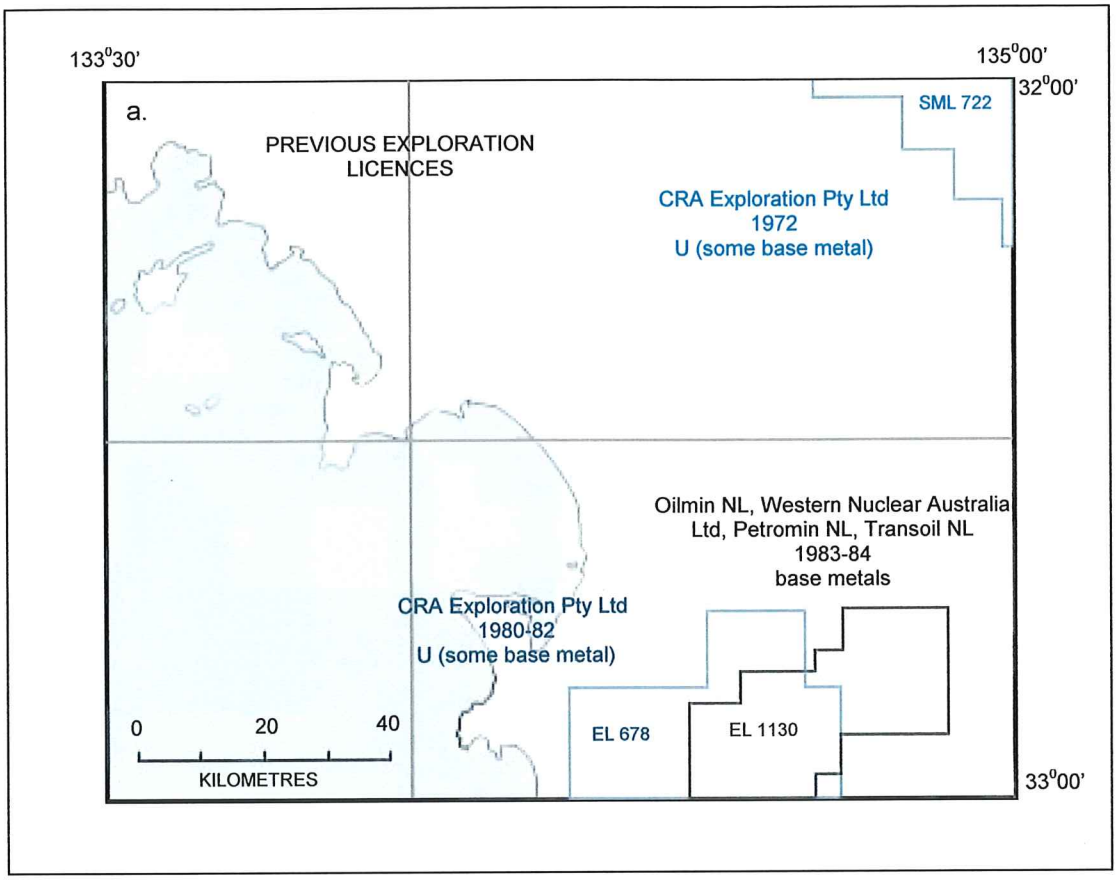
133°30'
135°00'
32°00'
a.
PREVIOUS EXPLORATION LICENCES
SML 722
CRA Exploration Pty Ltd
1972
U (some base metal)
Oilmin NL, Western Nuclear Australia Ltd, Petromin NL, Transoil NL
1983-84
base metals
CRA Exploration Pty Ltd
1980-82
U (some base metal)
EL 678
EL 1130
0
20
40
KILOMETRES
33°00'

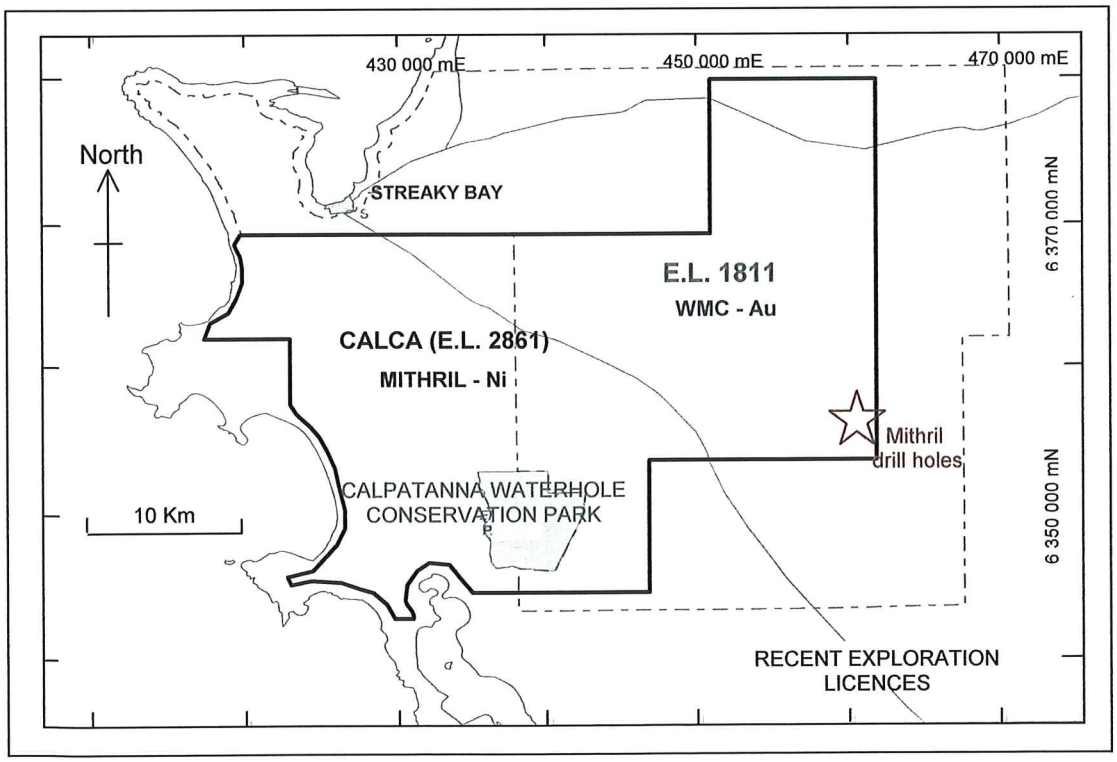
430 000 mE
450 000 mE
470 000 mE
North
STREAKY BAY
E.L. 1811
WMC - Au
CALCA (E.L. 2861)
MITHRIL - Ni
Mithril drill holes
6 370 000 mN
6 350 000 mN
10 Km
CALPATANNA WATERHOLE CONSERVATION PARK
RECENT EXPLORATION LICENCES

Fig. 6a & b.

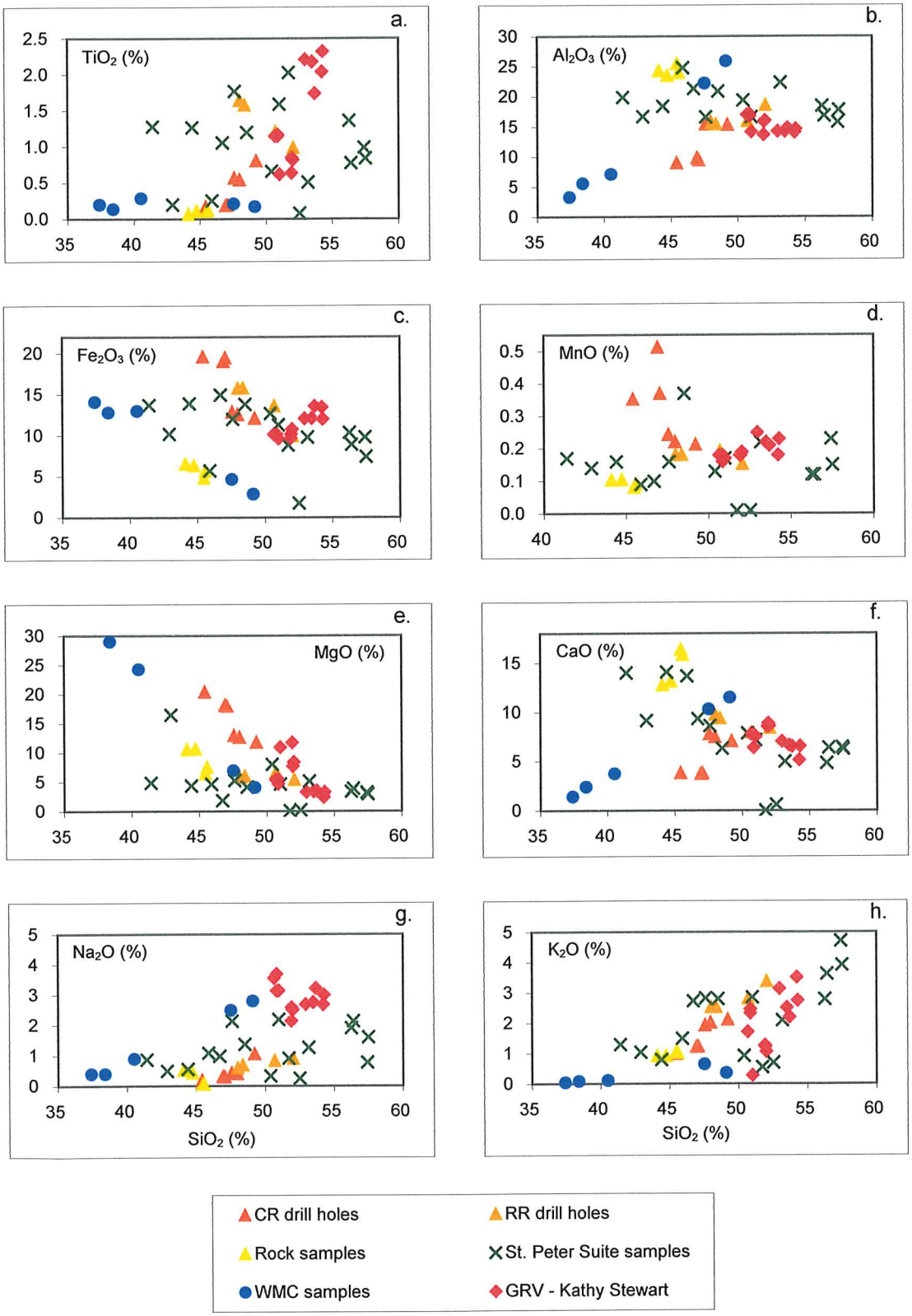
a.
TiO2 (%)
b.
Al2O3 (%)
c.
Fe2O3 (%)
d.
MnO (%)
e.
MgO (%)
f.
CaO (%)
g.
Na2O (%)
SiO2 (%)
h.
K2O (%)
SiO2 (%)
CR drill holes
RR drill holes
Rock samples
St. Peter Suite samples
WMC samples
GRV - Kathy Stewart

Fig. 7a-h.

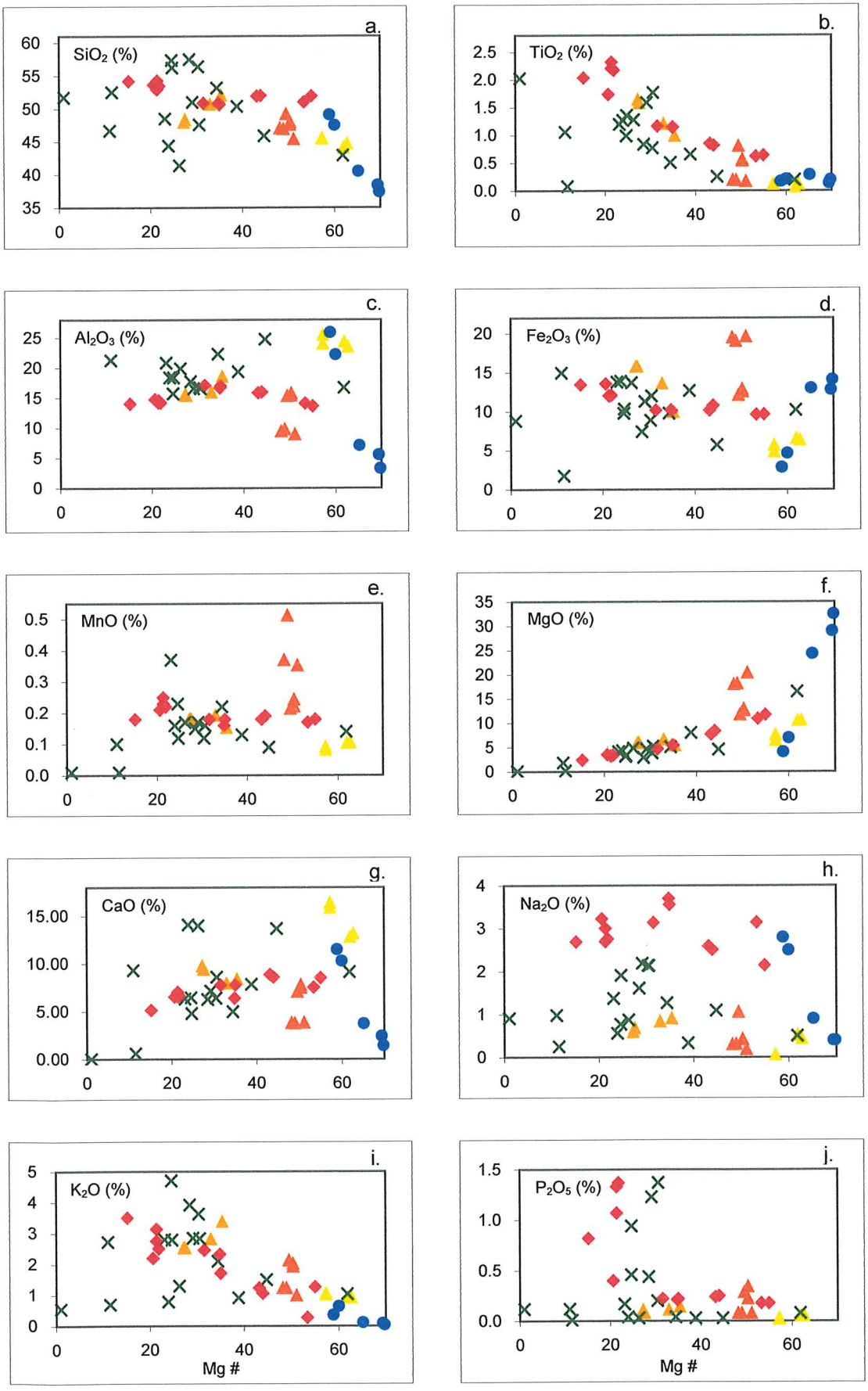
a.
SiO2 (%)
b.
TiO2 (%)
c.
Al2O3 (%)
d.
Fe2O3 (%)
e.
MnO (%)
f.
MgO (%)
g.
CaO (%)
h.
Na2O (%)
i.
K2O (%)
Mg #
j.
P2O5 (%)
Mg #

Fig. 8a-j.

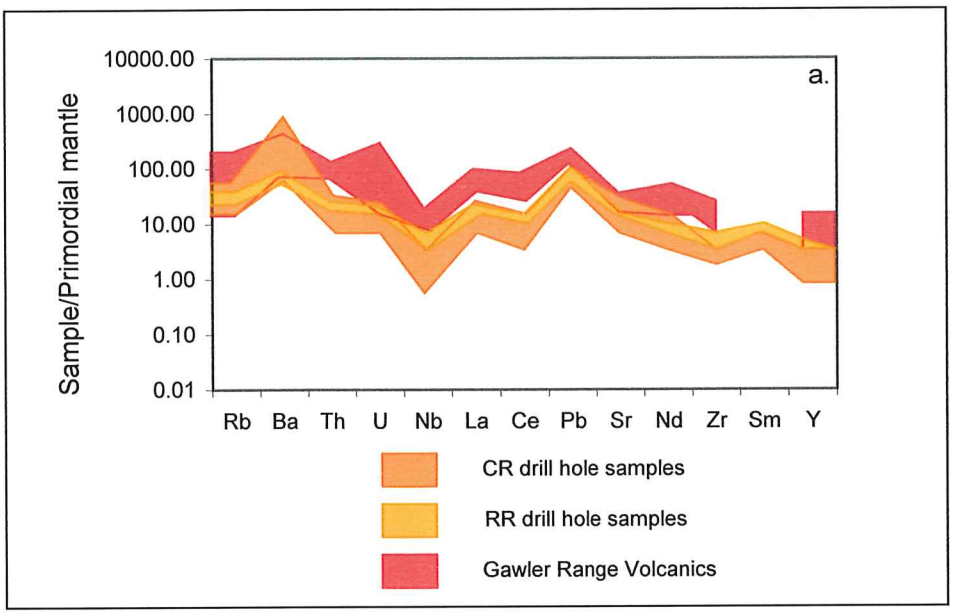
a.
Sample/Primordial mantle
10000.00
1000.00
100.00
10.00
1.00
0.10
0.01
Rb Ba Th U Nb La Ce Pb Sr Nd Zr Sm Y
CR drill hole samples
RR drill hole samples
Gawler Range Volcanics

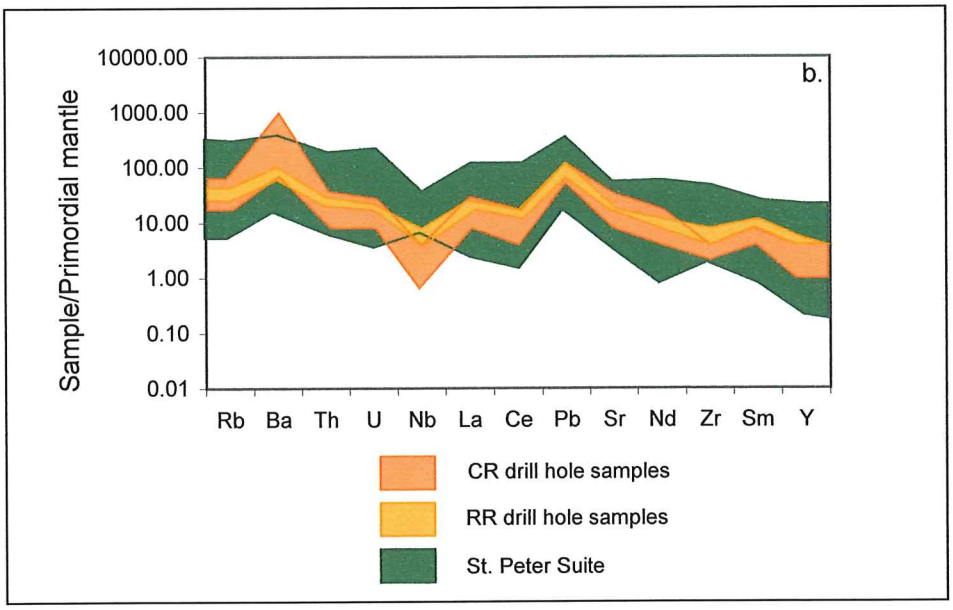
b.
Sample/Primordial mantle
10000.00
1000.00
100.00
10.00
1.00
0.10
0.01
Rb Ba Th U Nb La Ce Pb Sr Nd Zr Sm Y
CR drill hole samples
RR drill hole samples
St. Peter Suite

Fig. 9a & b.

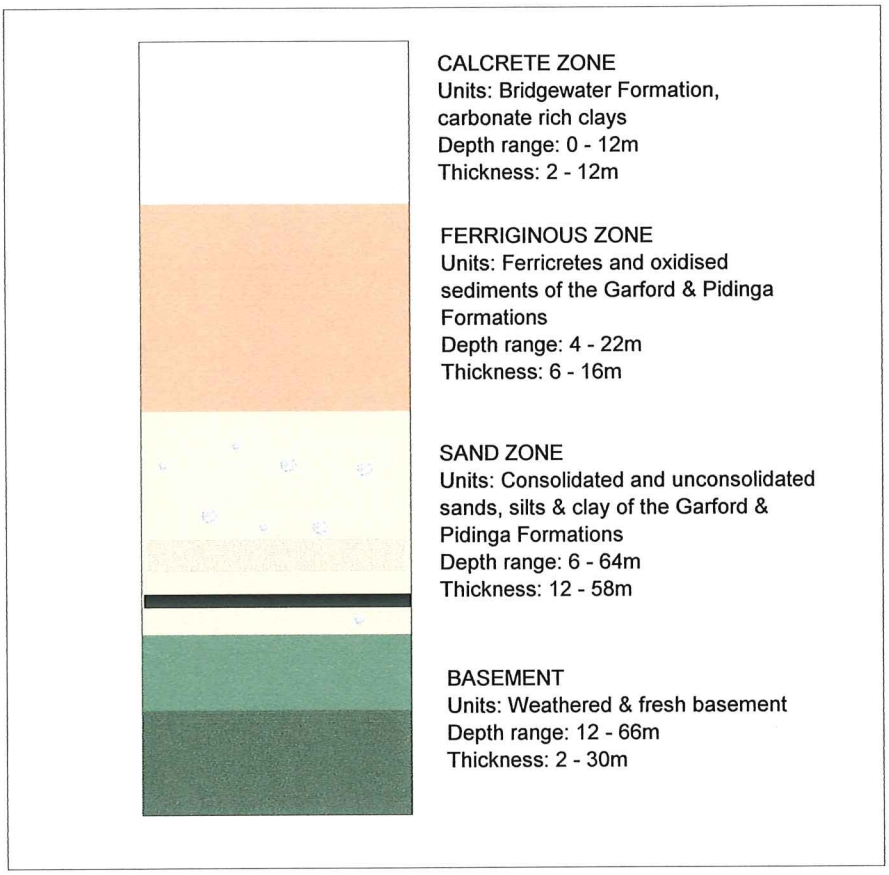
CALCRETE ZONE
Units: Bridgewater Formation, carbonate rich clays
Depth range: 0 - 12m
Thickness: 2 - 12m
FERRIGINOUS ZONE
Units: Ferricretes and oxidised sediments of the Garford & Pidinga Formations
Depth range: 4 - 22m
Thickness: 6 - 16m
SAND ZONE
Units: Consolidated and unconsolidated sands, silts & clay of the Garford & Pidinga Formations
Depth range: 6 - 64m
Thickness: 12 - 58m
BASEMENT
Units: Weathered & fresh basement
Depth range: 12 - 66m
Thickness: 2 - 30m

Fig. 10.

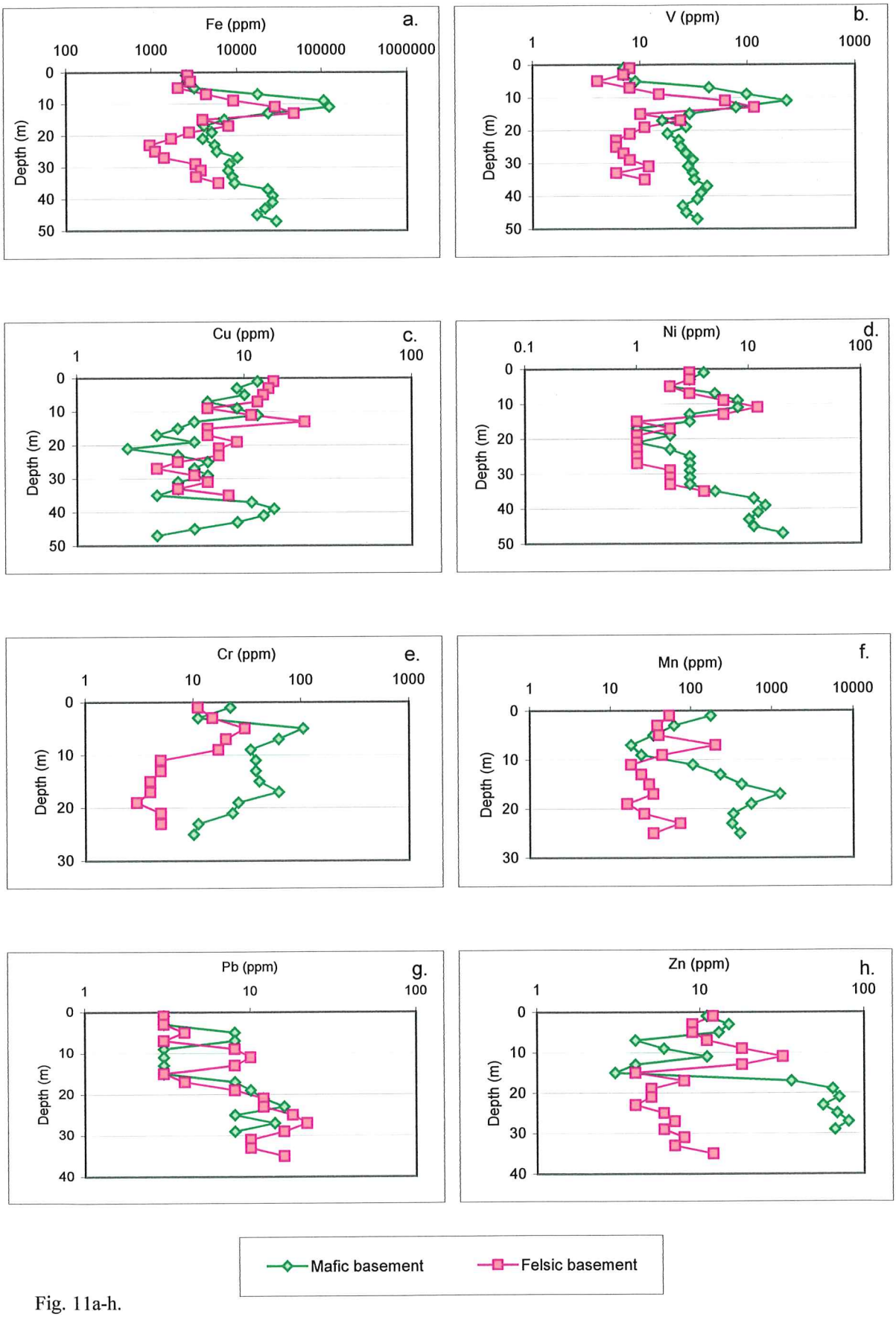
a.
Fe (ppm)
100
1000
10000
100000
1000000
b.
V (ppm)
1
10
100
1000
c.
Cu (ppm)
1
10
100
d.
Ni (ppm)
0.1
1
10
100
e.
Cr (ppm)
1
10
100
1000
f.
Mn (ppm)
1
10
100
1000
10000
g.
Pb (ppm)
1
10
100
h.
Zn (ppm)
1
10
100
Depth (m)
Mafic basement
Felsic basement

Fig. 11a-h.

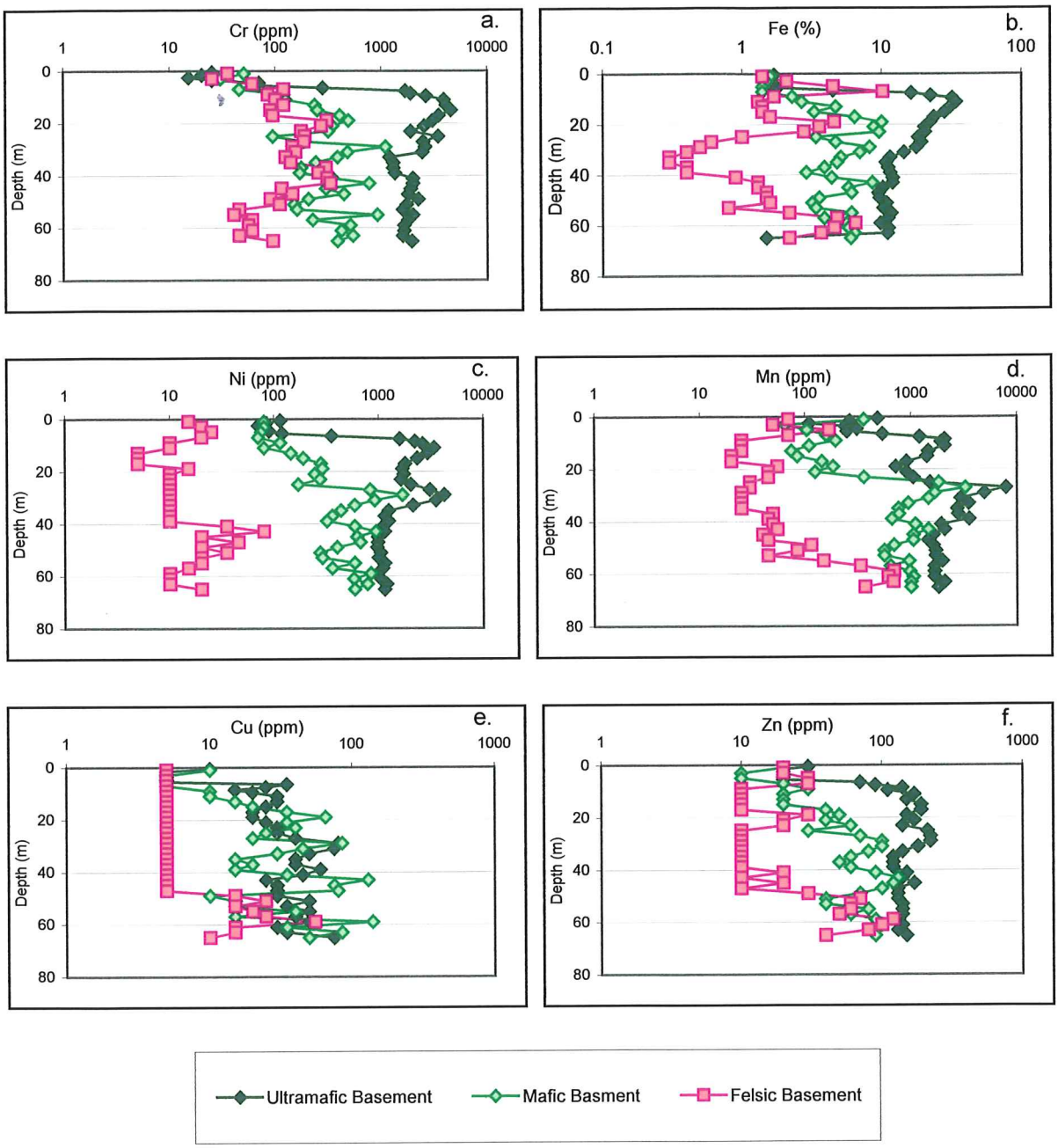
a.
Cr (ppm)
1
10
100
1000
10000
b.
Fe (%)
0.1
1
10
100
c.
Ni (ppm)
d.
Mn (ppm)
e.
Cu (ppm)
f.
Zn (ppm)
Depth (m)
0
20
40
60
80
Ultramafic Basement
Mafic Basment
Felsic Basement

Fig. 12a-f.

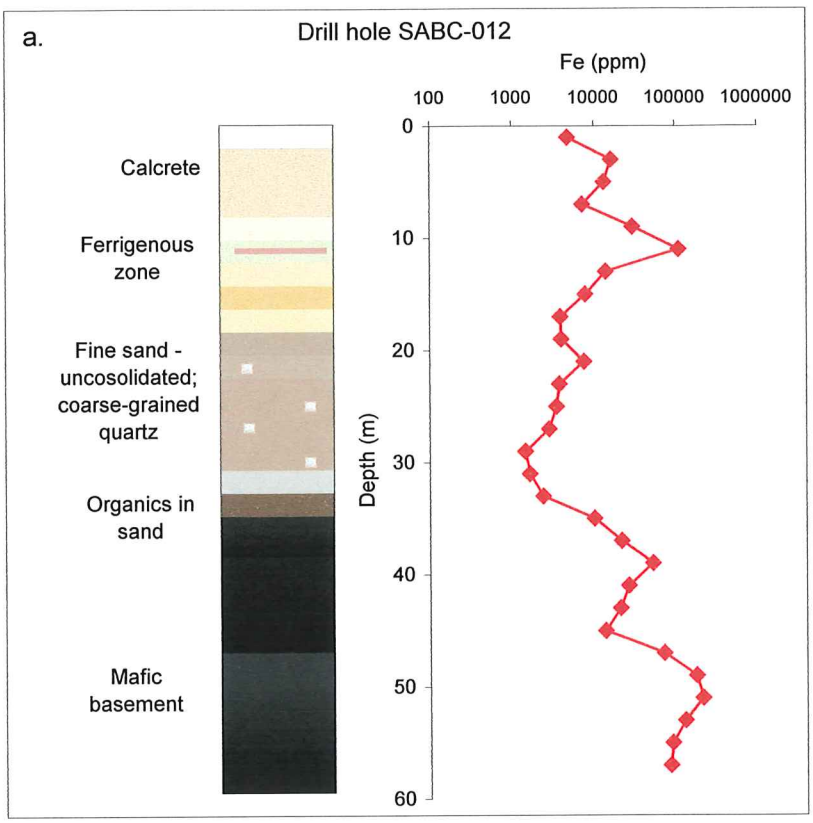
a.
Drill hole SABC-012
Fe (ppm)
100
1000
10000
100000
1000000
0
10
20
30
40
50
60
Depth (m)
Calcrete
Ferrigenous zone
Fine sand - uncosolidated; coarse-grained quartz
Organics in sand
Mafic basement

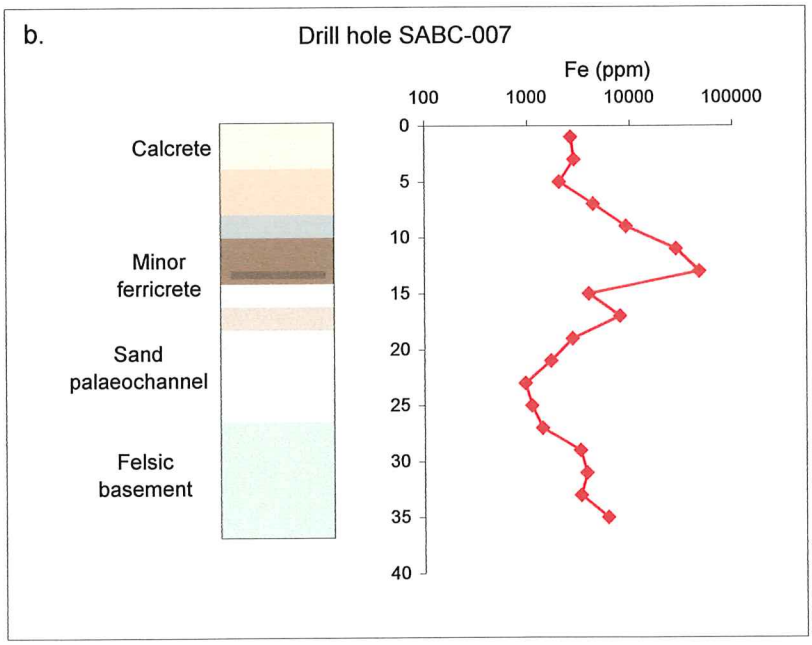
b.
Drill hole SABC-007
Fe (ppm)
100
1000
10000
100000
0
5
10
15
20
25
30
35
40
Calcrete
Minor ferricrete
Sand palaeochannel
Felsic basement

Fig. 13a & b.

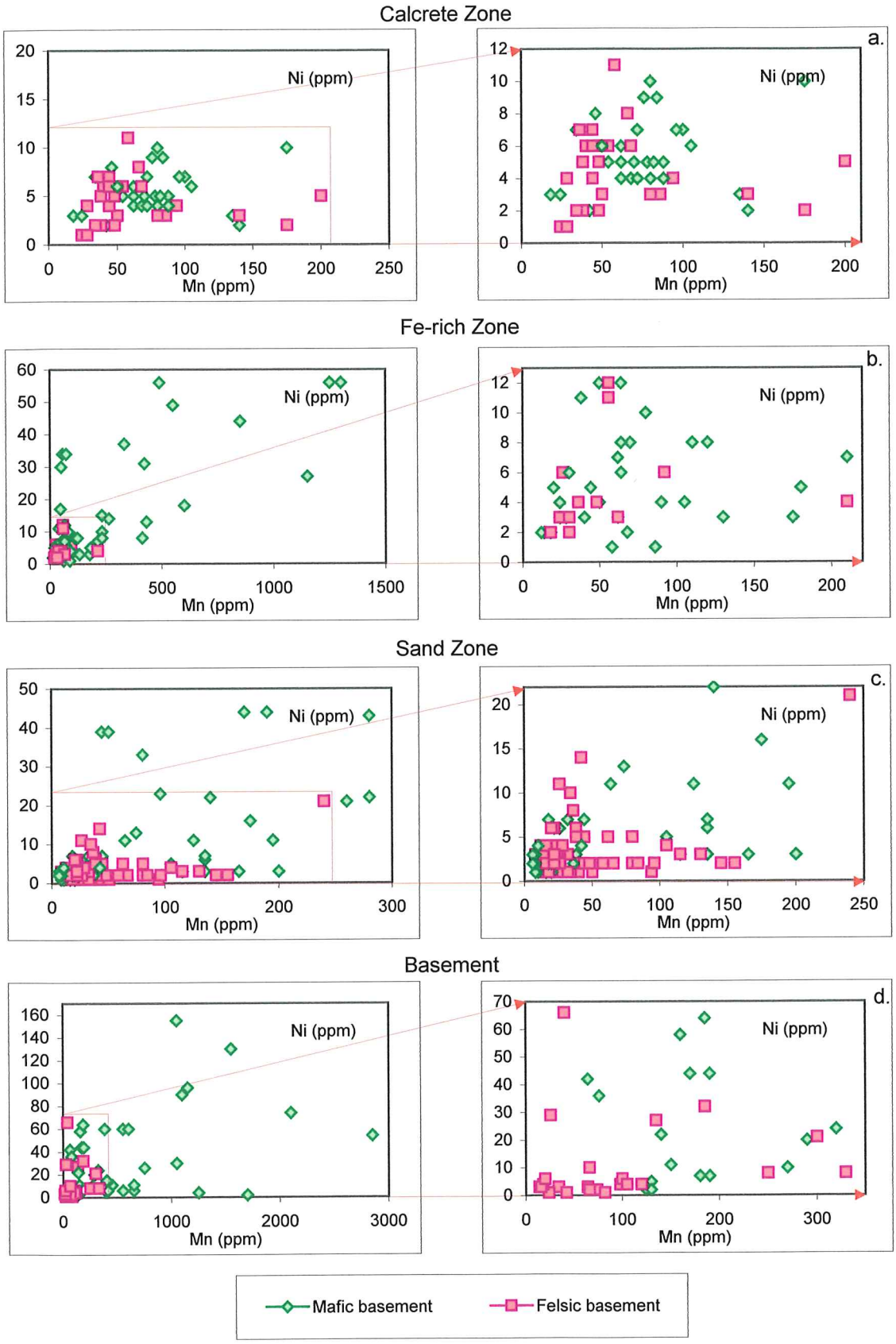
Calcrete Zone
Ni (ppm)
Mn (ppm)
a.
Fe-rich Zone
b.
Sand Zone
c.
Basement
d.
Mafic basement
Felsic basement

Fig. 14a-d.

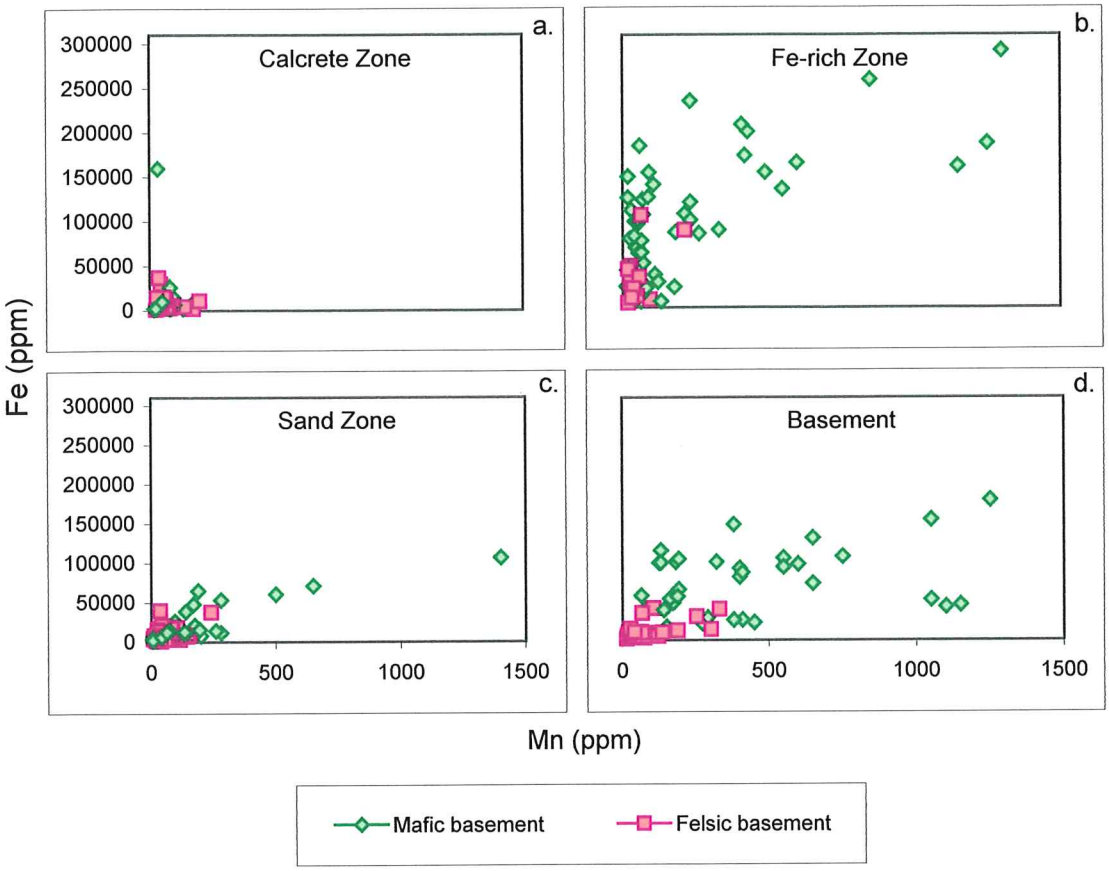
a.
Calcrete Zone
b.
Fe-rich Zone
c.
Sand Zone
d.
Basement
300000
250000
200000
150000
100000
50000
0
0
500
1000
1500
Fe (ppm)
Mn (ppm)
Mafic basement
Felsic basement

Fig. 15a-d.

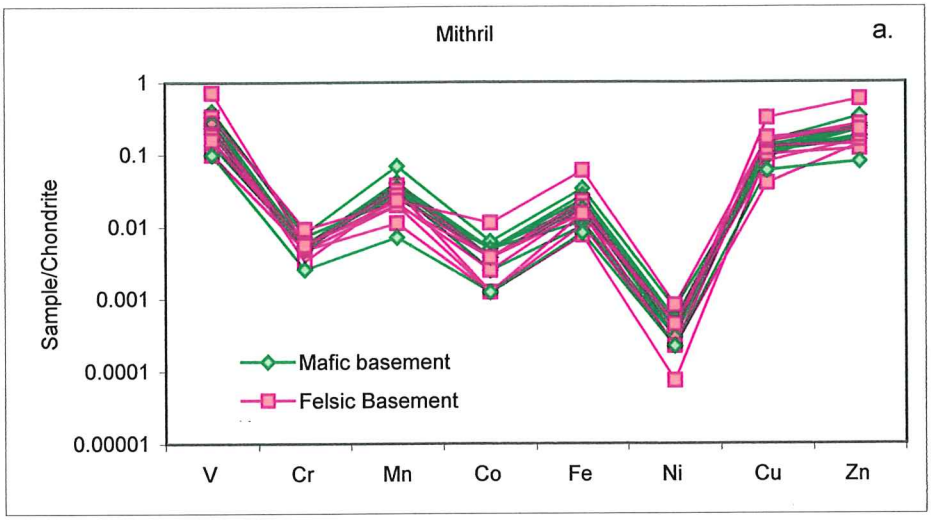
Mithril
a.
Sample/Chondrite
1
0.1
0.01
0.001
0.0001
0.00001
Mafic basement
Felsic Basement
V
Cr
Mn
Co
Fe
Ni
Cu
Zn

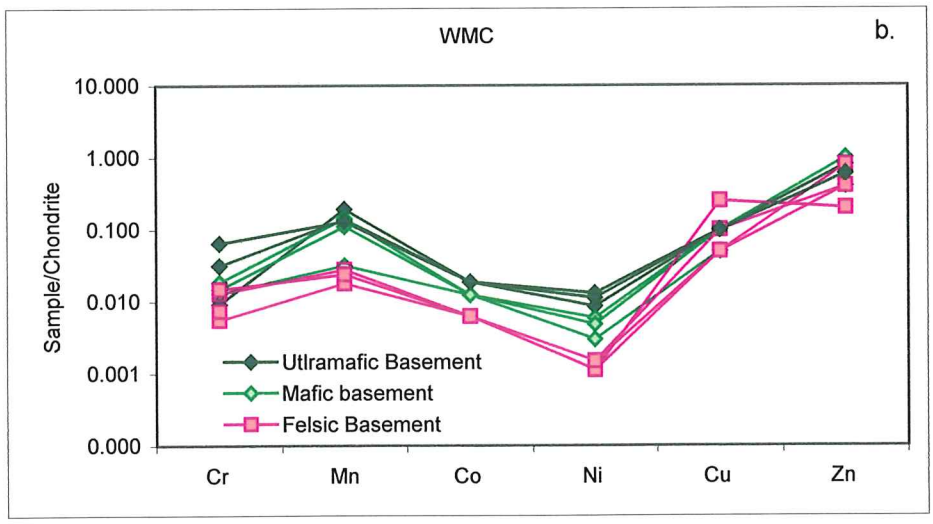
WMC
b.
Sample/Chondrite
10.000
1.000
0.100
0.010
0.001
0.000
Utlramafic Basement
Mafic basement
Felsic Basement
Cr
Mn
Co
Ni
Cu
Zn

Fig. 16a & b.

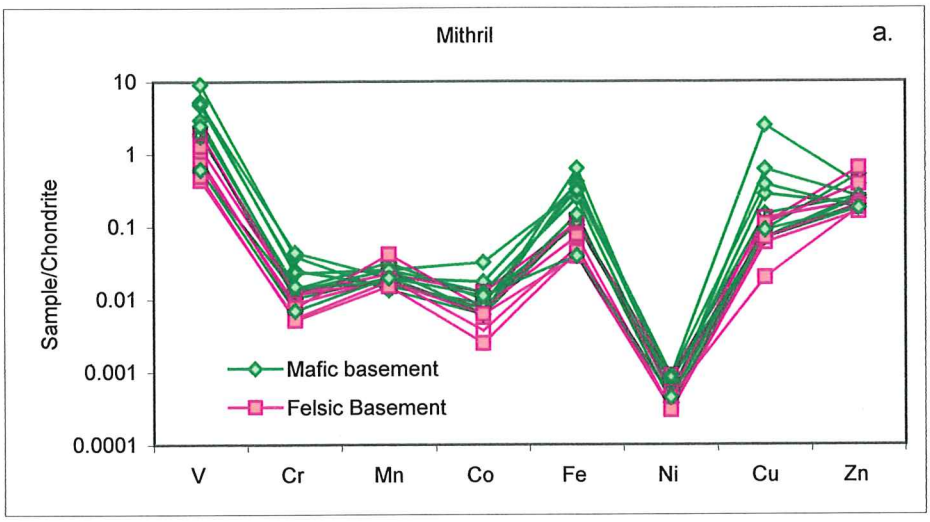
Mithril
a.
10
1
0.1
0.01
0.001
0.0001
Sample/Chondrite
Mafic basement
Felsic Basement
V
Cr
Mn
Co
Fe
Ni
Cu
Zn

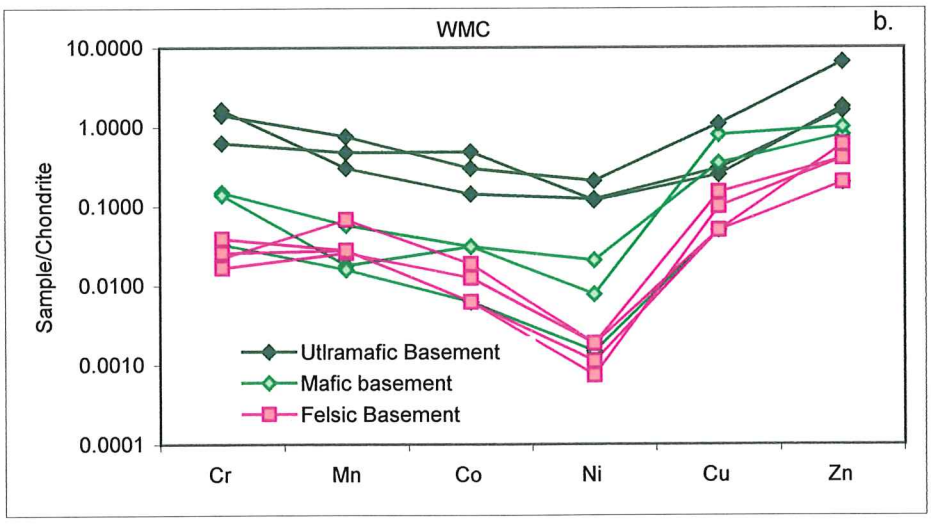
WMC
b.
10.0000
1.0000
0.1000
0.0100
0.0010
0.0001
Sample/Chondrite
Utlramafic Basement
Mafic basement
Felsic Basement
Cr
Mn
Co
Ni
Cu
Zn

Fig. 17a & b.

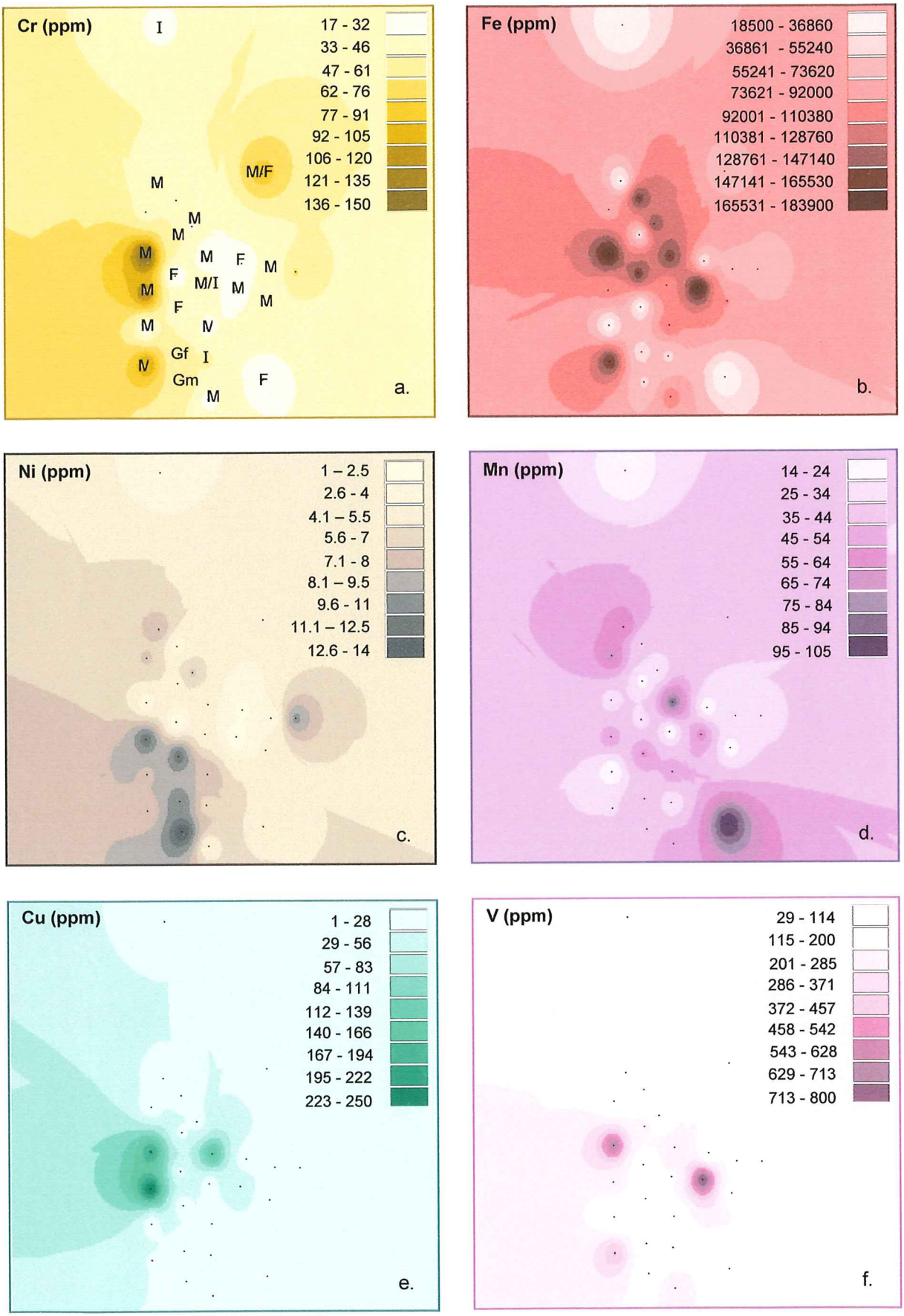

M – Mafic, I – Intermediate, F – felsic, Gm – Mafic Gneiss, Gf – Felsic Gneiss

Fig. 18a-f.

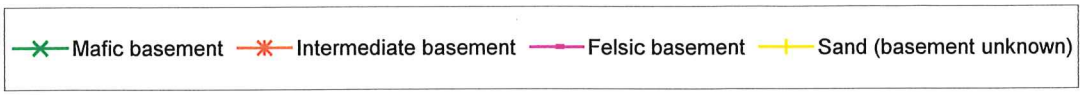

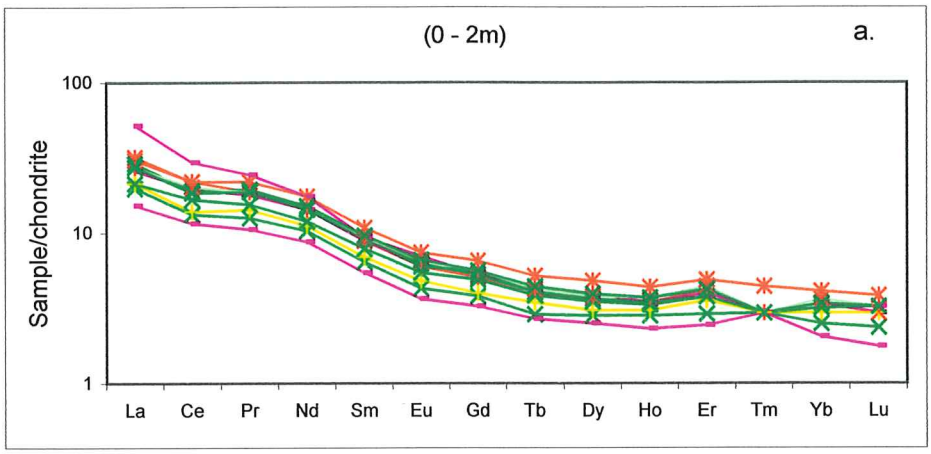

Figure 15a.

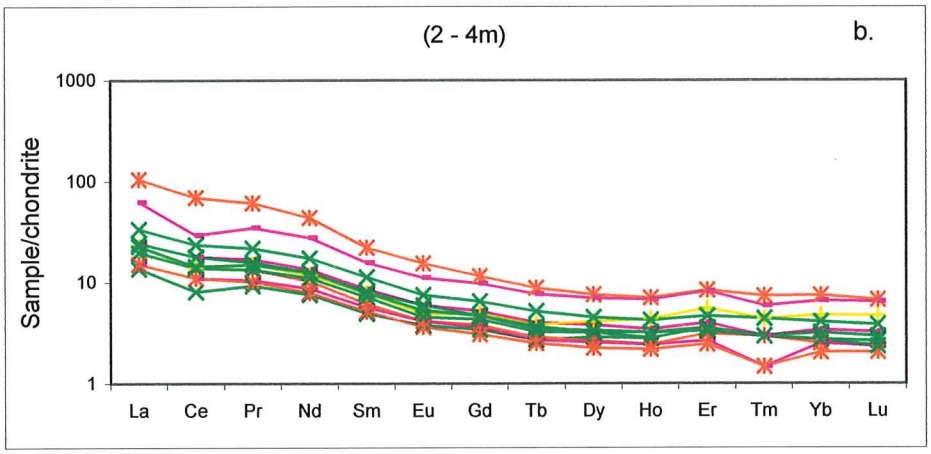

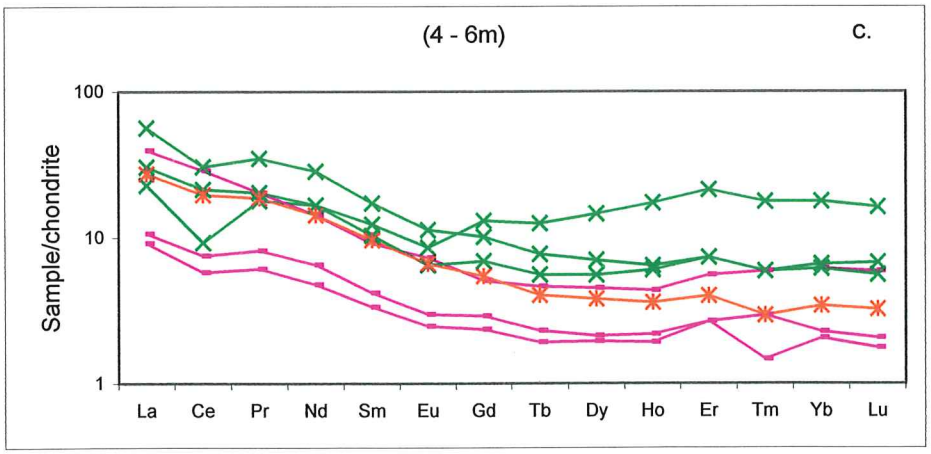

Fig. 19a-c.

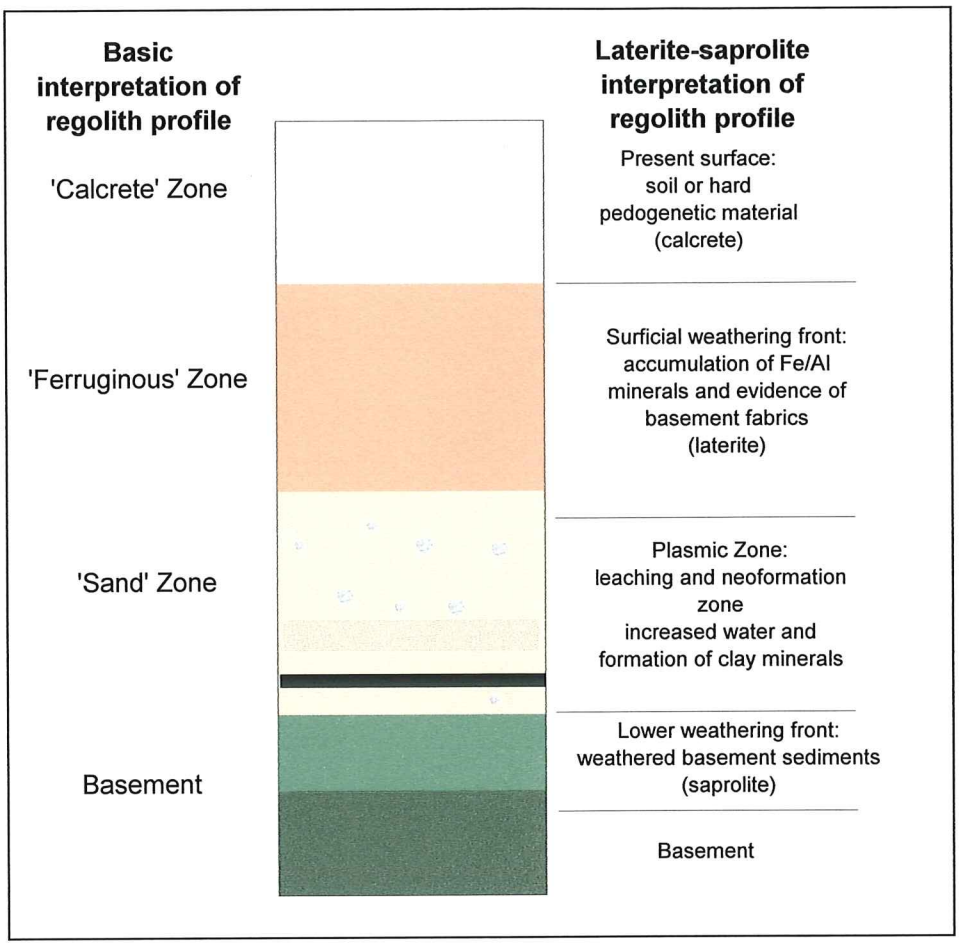
Basic interpretation of regolith profile
'Calcrete' Zone
'Ferruginous' Zone
'Sand' Zone
Basement
Laterite-saprolite interpretation of regolith profile
Present surface: soil or hard pedogenetic material (calcrete)
Surficial weathering front: accumulation of Fe/Al minerals and evidence of basement fabrics (laterite)
Plasmic Zone: leaching and neoformation zone increased water and formation of clay minerals
Lower weathering front: weathered basement sediments (saprolite)
Basement

Fig. 20